Dissertation

submitted to the

Combined Faculties for the Natural Sciences
and for Mathematics
Ruperto-Carola University of Heidelberg, Germany

for the degree of
Doctor of Natural Sciences

presented by
Diplom-Biologist Claus Rieker

born in Geislingen / Steige

oral examination:

Dissecting nucleolar functions in dopaminergic neurons and Parkinson's disease by targeted inactivation of the transcription-initiation factor IA (TIF-IA)

Referees:

Prof. Dr. Günther Schütz
Prof. Dr. Hilmar Bading

Table of contents

1. Summary

The most prominent neurodegenerative disorder associated with dopaminergic cell loss is Parkinson's disease (PD). The main hallmark of PD is the progressive loss of substantia nigra neurons. The neuronal loss results in severe dopamine depletion in the striatum, responsible for the motor symptoms associated with PD, especially tremor, rigidity and bradykinesia. Although the pathological changes that characterize the disease are well documented, the mechanism responsible for the death of dopaminergic neurons remains to be unraveled. However, studies showed that oxidative stress is of major importance in the etiology of the disease. In order to efficiently respond to hazardous conditions, cellular stress sensors are required, like the nucleolus, which responds to cellular stress by stabilizing the transcription factor p53. Therefore, the aim of the present study was the analysis of the importance of the nucleolar function in the oxidative stress response in dopaminergic neurons and its implications in the etiology of PD.

The main function of the nucleolus, a sub-organelle of the cell nucleus, is the production and assembly of ribosome components. Nucleoli are made of protein and ribosomal DNA (rDNA) sequences of chromosomes, which serves as the template for transcription of the ribosomal RNA (rRNA) for inclusion in new ribosomes. Following increased oxidative stress in dopaminergic neurons by 1-methyl-4-phenyl-1,2,3,6-tetrahydropyridin (MPTP) treatment, impairment of nucleolar structure and reduced nucleolar activity (RNA polymerase I) was discernible. The key player in the regulation of rDNA transcription is the transcription initiation factor IA (TIF-IA), which is responsible for the adjustment of cell biosynthetic activities to environmental conditions. In order to elucidate the role of the nucleolus within dopaminergic neurons, the Cre/loxP recombination system was used to generate mouse mutants, in which the function of the nucleolus was artificially disrupted by the ablation of TIF-IA in dopaminergic neurons (TIF-IA^{DATCre}). The impairment of nucleolar function leads to progressive loss of dopaminergic neurons, reduction of the striatal dopamine content and severely impaired locomotor performance, closely mimicking the symptoms in PD. Remarkably, nucleolar disruption causes mitochondrial impairment before structural changes in dopaminergic neurons or their projections to the striatum were observed.

To assess in more detail how nucleolar disruption affects mitochondrial function, mutant mice expressing an inducible Cre recombinase have been generated, allowing the spatio-temporal control of the Cre-mediated TIF-IA ablation. By means of Cre reporter mice reliable expression of the Cre recombinase was ensured specifically in dopaminergic neurons and very low background activity of the transgene in absence of the ligand was detected. Activation of the Cre-mediated TIF-IA ablation in 2 months old animals (TIF-IA^{DATCreERT2}) leads to perturbation of nucleolar function followed by upregulation of p53, accompanied with mitochondrial dysfunction, leading to increased oxidative stress and finally to progressive loss of dopaminergic neurons. Treatment of TIF-IA^{DATCreERT2} and control mice with MPTP showed that an intact nucleolus is crucial for the balancing of the oxidative insult. The study was complemented by the analysis of PD samples in which increased nucleolar disruption could be observed. The results show the importance of nucleolar activity in the oxidative stress response in dopaminergic neurons, reveal a relationship between nucleolar and mitochondrial function, providing a new animal model for PD research and offer a new perspective on the neurodegenerative process of PD.

1.1 Zusammenfassung

Die bekannteste neurodegenerative Krankheit, welche mit dem Verlust von dopaminergen Neuronen zusammenhängt, ist die Parkinsonsche Erkrankung. Das Hauptmerkmal dieser Krankheit ist der langsam fortschreitende Verlust der dopaminergen Neuronen. Dieser Verlust führt zu einer Verminderung der Dopaminkonzentration im Striatum, welche verantwortlich ist für motorische Störungen wie Muskelstarre, Muskelzittern und Bewegungsarmut. Obwohl die pathologischen Veränderungen sehr genau beschrieben sind, ist der zugrundeliegende Mechanismus nicht bekannt. Jedoch haben Studien gezeigt, dass erhöhter oxidativer Stress in dopaminergen Neuronen die Schlüsselrolle bei der Entstehung der Parkinsonschen Krankheit einnimmt. Zellen registrieren diesen Stress mit Hilfe spezifischer Sensoren wie bspw. des Nukleolus, welcher auf wachsenden oxidativen Stress mit der Stabilisierung des Transkriptionsfaktor p53 reagiert. Das Ziel dieser Arbeit ist, die Funktion des Nukleolus in dopaminergen Neuronen bei der oxidativen Stress-Antwort zu ermitteln, sowie dessen Rolle bei der Parkinsonschen Erkrankung.

Durch das Nervengift 1-Methyl-4-phenyl-1,2,3,6-tetrahydropyridin (MPTP) ausgelöste Erhöhung des oxidativen Stress, führte zu einer Beeinträchtigung der nucleolären Struktur sowie zu einer starken Reduktion der Transkriptionsrate der ribosomalen DNA. Es wurde gezeigt, dass die Regulation der rDNA-Transkription hauptsächlich durch den Transkriptions-Initiations-Faktor-IA (TIF-IA) erfolgt, welcher für die Abstimmung der biosynthetischen Aktivität der Zelle auf die jeweiligen Umgebungsbedingungen verantwortlich ist. Um die Funktionen des Nukleolus dabei näher untersuchen zu können, wurden Mausmutanten mit Hilfe des Cre/loxP Rekombinationssystems erzeugt (TIF-IA^{DATCre}), bei denen die Funktion des Nukleolus durch die Inaktivierung des TIF-IA Gens in dopaminergen Neuronen beeinträchtigt wurde. Diese Mutation führte zu einem langsamen Absterben der dopaminergen Neurone, reduziertem Dopamingehalt im Striatum und einer daraus resultierenden beeinträchtigten Motorik, welche die Symptome der Parkinsonschen Erkrankung widerspiegelt.

Bemerkenswerterweise führt der Verlust von nukleolärer Funktion zu einer direkten Beeinträchtigung der mitochondrialen Aktivität, weit früher als die ersten strukturellen Veränderungen sichtbar werden. Um diese Sachlage näher analysieren zu können, wurden Mausmutanten, in denen zu einem festgelegten Zeitpunkt die Inaktivierung des TIF-IA Gens erfolgt, hergestellt (TIF-IA^{DATCreERT2}). Unter Zuhilfenahme einer Cre Reporter Mauslinie wurde die hohe Spezifität der Expression des Transgenes (DATCreER^{T2}), sowie dessen geringe Hintergrundaktivität nachgewiesen. Die Aktivierung des Ablationssystems führt zu einer Beeinträchtigung der nukleolären Funktionen, dann zu p53 Hochregulation, gefolgt von mitochondrialer Beeinträchtigung und steigendem oxidativen Stress, welcher schließlich zu einem progressiven Verlust von dopaminergen Neuronen führte. Ferner wurde durch TIF-IA^{DATCreERT2} und Kontrollmäuse, welche mit MPTP zwei Wochen nach Aktivierung des Ablationssystems behandelt wurden, gezeigt, dass zur Kompensation von oxidativem Stress ein intakter Nukleolus notwendig ist. Des Weiteren ergab die Analyse von Gewebe von Parkinsonpatienten eine deutlich geringere Anzahl an intakten Nukleoli in dopaminergen Neuronen im direkten Vergleich mit Kontrollgewebe. Die Ergebnisse, welche hier präsentiert werden, zeigen die Bedeutung nukleolärer Aktivität bei der oxidativen Stress-Antwort in dopaminergen Neuronen, beschreiben eine Interaktion zwischen dem Nukleolus und dem Mitochondrium und liefern neue Mausmodelle bzw. Denkansätze für die Erforschung und das Verständnis der Parkinsonschen Erkrankung.

2. Introduction

2.1 Neural development

The development of the nervous system starts at a relatively late stage during embryogenesis after the three main cellular layers endoderm, mesoderm and ectoderm have been developed. The ectoderm develops into the major tissues of central and peripheral nervous systems. After the process of neurulation, in which the neural plate folds into a tubular structure, called neural tube, the caudal region of the neural tube gives rise to the spinal cord while the rostral part becomes the brain. Through this early stage, rapidly proliferating cells form three brain vesicles: the forebrain (prosencephalon), the midbrain (mesencephalon) and the hindbrain (rhombencephalon). The differentiation of cells in the nervous system is the consequence of a complex program that directs the expression of specific genes in individual cells. In the last phases of this program the development of dopaminergic neurons occurs (Principles of neural science 4th edition; Fundamental Neuroscience 2nd edition; Molecular biology of the cell 3rd edition).

2.2 Dopaminergic neurons

Dopaminergic neurons are an anatomically and functionally heterogeneous group of cells, localized in the forebrain, midbrain and the olfactory bulb. The most prominent dopaminergic cell group resides in the ventral part of mesencephalon, which contains approximately 90% of the total number of brain dopaminergic cells. The mesencephalic dopaminergic system has been subdivided into several systems (Fig. 1). Prominent among is the nigrostriatal system, which originates in the zona compacta of the substantia nigra (Fig. 1 – light blue) and extends its fibers in the caudate-putamen (also known as the dorsal striatum). The nigrostriatal pathway plays an essential role in the control of voluntary motor movement. More medial to this pathway are the mesolimbic and mesocortical dopaminergic systems, which arise from dopaminergic cells residing in the ventral tegmental area (VTA) (Fig. 1 - blue). These systems are involved in emotion-based behavior including motivation

and reward. The cells of the VTA project most prominently into the nucleus accumbens, olfactory tubercle but also innervate the septum, amygdala and hippocampus. This subset of the projections is known as the mesolimbic dopaminergic system. Cells of the medial VTA project to the prefrontal, cingulate and perirhinal cortex. This pathway is known as the mesocortical dopaminergic system. There is considerable overlap between the VTA cells that project to these various targets. Because of the overlap between the mesocortical and mesolimbic dopaminergic neurons, the two systems are often collectively referred to as the mesocorticolimbic system.

The tuberoinfundibular pathway transmits dopamine from the hypothalamus to the pituitary gland (Fig. 1 – dark blue). This pathway influences the secretion of certain hormones, including prolactin (Principles of neural science 4th edition; Wise, 2004).

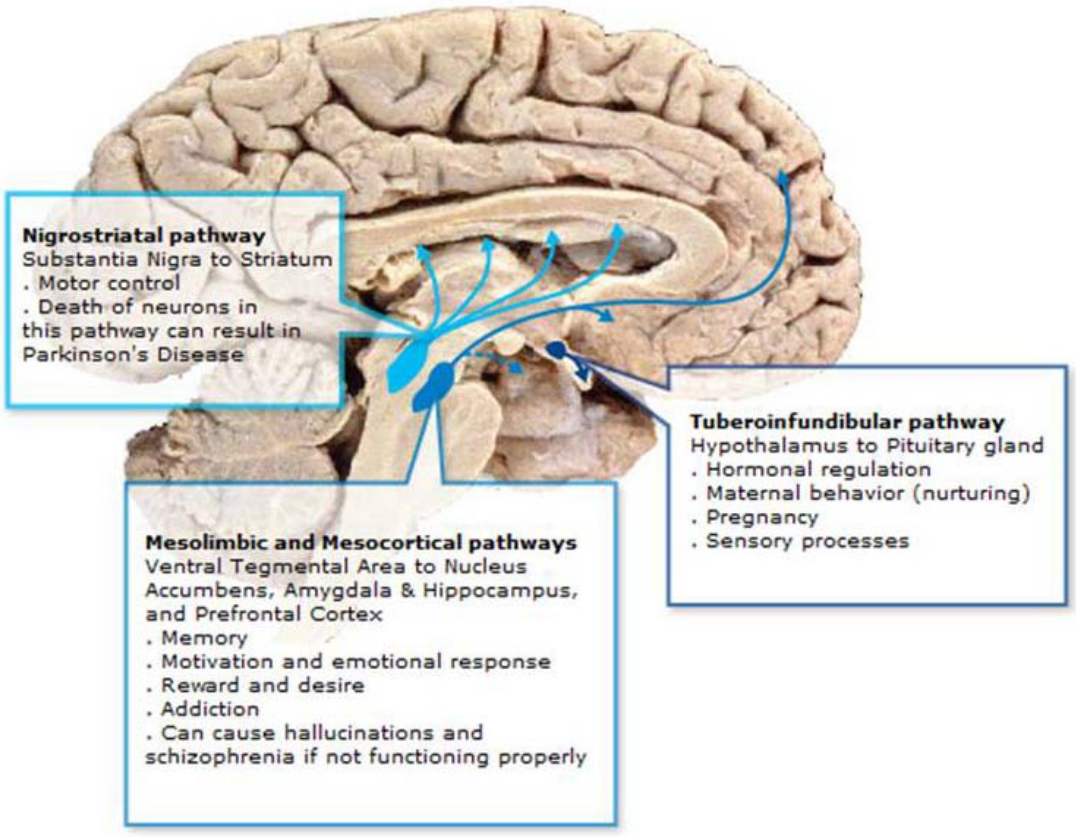

Figure 1: The different dopaminergic pathways in human brain
(Adapted from BrainNet)

2.3 Dopamine and associated cellular pathologies

Considerable differences exist in the numbers of dopaminergic cell bodies in various mammals ranging from about 30.000 in the mouse (total number: $7{,}5x10^7$ neurons), or 590.000 in humans (total number: 10^{11} neurons) (German and Manaye, 1993). Although dopaminergic neurons correspond to less than 1% of the total number of brain neurons, they nevertheless play an important role in regulating numerous aspects of basic brain function, like motor behavior, motivation and working memory. Hence, the regulation of dopamine plays a crucial role in both mental and physical health (Wise, 2004).
In 1952, Arvid Carlsson and colleagues discovered dopamine. They found that dopamine is not just a precursor of norepinephrine and epinephrine but acts as a neurotransmitter as well (Benes, 2001). In the brain, dopamine functions as a neurotransmitter, activating five different types of dopamine receptors (D1-D5), whereas dopamine released by the hypothalamus acts as neurohormone, by inhibition of the prolactin release from the anterior lobe of the pituitary. As a member of the catecholamine family (includes substances consisting of catechol: aromatic structure with two hydroxyl groups), dopamine is a precursor to norepinephrine and epinephrine in the biosynthetic pathways for these neurotransmitters.
Dopamine is biosynthesized in the body (mainly by nervous tissue and the medulla of the adrenal glands) first by the hydration of the amino acid L-tyrosine to L-DOPA (L-3,4-dihydroxyphenylalanine) via the enzyme tyrosine hydroxylase followed by the decarboxylation of L-DOPA by aromatic L-amino acid decarboxylase (Fig. 2). Dopamine is thought to be capable of generating toxic reactive oxygen species (ROS) via both its enzymatic and non-enzymatic catabolism (Halliwell, 1992). Specifically, dopamine oxidation can occur either spontaneously in the presence of transition metal ions or via an enzyme-catalyzed reaction involving the monoamine oxidase (MAO). Oxidation of dopamine via MAO generates a spectrum of toxic species including H_2O_2, oxygen radicals, semiquinones, and quinones (Graham, et al., 1978). At the same time dopaminergic neurons are known to be particularly prone to oxidative stress most likely due to their high rate of oxygen

metabolism, low levels of antioxidants and high iron content (Dauer and Przedborski, 2003).

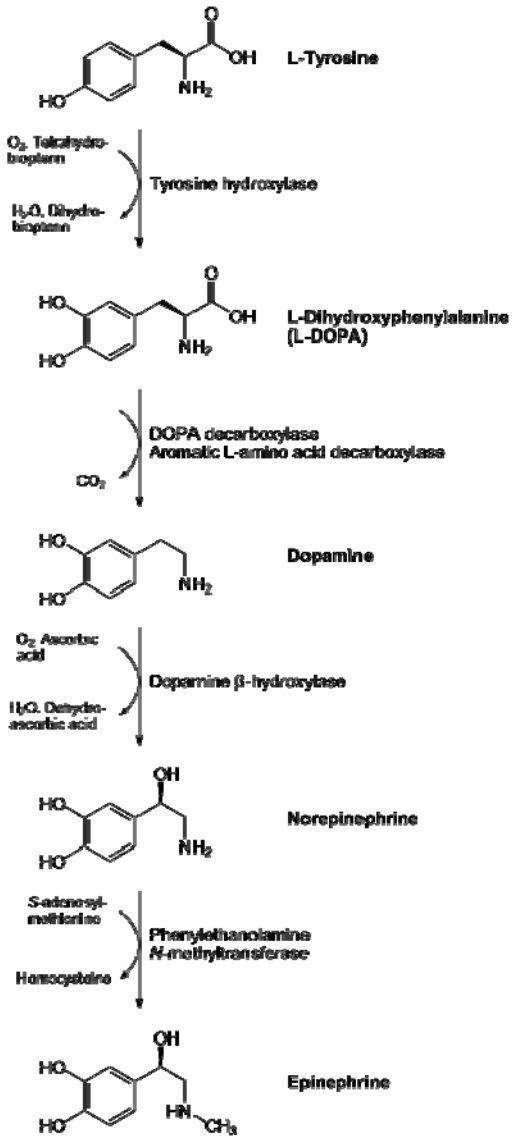

Figure 2: Biosynthesis of dopamine
(Adapted from Biochemistry 5th edition)

2.4 Parkinson's disease

The most prominent neurodegenerative disorders associated with dopaminergic cell loss is Parkinson's disease (PD). In PD, which was first described by James Parkinson in 1817, the loss of nigral neurons follows a specific pattern with the more susceptible area being located laterally in the ventral part of the substantia nigra (Parkinson, 2002). This results in severe dopamine depletion in the striatum, responsible for the motor symptoms associated with PD, especially bradykinesia (slowness of movement), tremor, rigidity and loss of postural control (Lang and Lozano, 1998b, Lang and Lozano, 1998a). Other less severe lesions, such as degeneration of the dopaminergic VTA, the noradrenergic locus coeruleus and the ascending cholinergic pathway from the Meynert basalis nucleus are also observed (Candy, et al., 1983). Additionally, dopaminergic cell loss can be associated with the presence of eosinophilic intraneuronal inclusions, called Lewy bodies, composing of alpha-synuclein, parkin and ubiquitin (Goldman, et al., 1983).

Although the pathological changes and motor dysfunction that characterize the disease are well documented, the mechanism responsible for the death of dopaminergic neurons remains to be unraveled. Therefore, most of the current treatment for the disease is largely symptomatic. So far, the most commonly prescribed drug for PD is the DA precursor L-DOPA (Birkmayer and Hornykiewicz, 1961). It is used as treatment for PD patients to replace lost midbrain dopamine. Unfortunately, L-DOPA and other parkinsonian drugs are only able to alleviate the symptoms of the disease but not ongoing cell death and eventually become ineffective once enough dopaminergic neurons are lost. Moreover, many patients develop dyskinesia (abnormal involuntary movements) and motor fluctuations within a few years of L-DOPA treatment (Ahlskog and Muenter, 2001). L-DOPA-induced dyskinesia (LID) is the earliest and most common complication and is typically associated with an idiosyncratic mixture of chorea (abrupt movements that seem to flow from one body part to another) and dystonia (slow twisting movement) (Cenci, 2007).

Therefore there has been resurgence in the use of surgical techniques such as pallidotomy and thalamotomy in which lesions are made in the patient's

globus pallidus or thalamus, respectively, which was used before L-DOPA was discovered, to treat PD (Kashihara, 2007). Unfortunately, surgical treatment is not effective in PD patients. New experimental methods including deep brain stimulation, where electrodes stimulate the thalamus and implantation of stem cells in the striatum are currently under investigation (Lindvall and Kokaia, 2006, Kern and Kumar, 2007).

2.5 Molecular mechanism of PD

The major breakthrough in elucidating the etiology of the disease resulted from the accidental discovery of 1-methyl-4-phenyl-1,2,3,6-terahydropyridine (MPTP). In 1976, a chemistry graduate student was hospitalized after exhibiting Parkinson-like symptoms. It was found that the cause of his condition was injection of MPTP, a product of an incorrect reaction while trying to prepare a synthetic opioid. After his death, a selective destruction of dopamine neurons in the SN was discovered (Parkinson's disease 1st edition, S.A. Factor and W.J. Weiner). Due to the relatively selective degeneration of dopaminergic neurons MPTP-treatment of animals is the most commonly studied PD model (Przedborski and Vila, 2003) .

MPTP itself is not toxic and as a lipophilic compound it can cross the blood-brain barrier. Once inside the brain, MPTP is metabolized by glia cells into 1-methyl-4-phenylpyridinium (MPP+) and via high-affinity uptake of the dopamine transporter MPP+ enters dopaminergic neurons. MPP+ is a toxic compound that interferes with complex I of the respiratory electron transport chain, causing the buildup of free radicals and molecules that contribute to cell destruction (Schober, 2004). So it is not surprising that studies have first focused on the three types of cellular dysfunction that may be important in the pathogenesis of PD: oxidative stress, mitochondrial respiration defect and abnormal protein aggregation. This situation changed in 1997 with the discovery that mutations in the gene for alpha-synuclein cause an inherited form of PD. In the following years several additional PD-causing genes have

been identified including Parkin, Ubiquitin C-terminal hydrolase-L1 (UCH-L1), PTEN-induced kinase-1 (PINK1) and DJ-1 (PARK7) (Forman, et al., 2005).
So far the relationship between the molecular pathways modified by these disease-associated genes and previous identified factors (like mitochondrial dysfunction) remains to be elucidated. Nevertheless it seems that oxidative stress is of major importance in the etiology of the disease (Vila and Przedborski, 2003, Moore, et al., 2005, Abou-Sleiman, et al., 2006, Lin and Beal, 2006).
Certain neurotoxins (like MPTP, 6-OHDA, etc) are known to induce parkinsonism in humans (Dauer and Przedborski, 2003). The majority of these neurotoxins inhibit the respiratory chain in mitochondria, resulting in increased production of reactive oxygen species (ROS) like oxygen ions, free radicals or hydrogen peroxide, which may damage proteins, lipids and DNA, finally leading to cell death (Lotharius and Brundin, 2002). Consistent with mitochondrial damage and ROS accumulation playing a crucial role in PD, inherited forms of PD contain mutations in genes that protect dopaminergic neurons against oxidative stress, such as Parkin, DJ-1 and PTEN-induced kinase-1 (PINK1) (Abou-Sleiman, et al., 2006, Lin and Beal, 2006). Studies in Drosophila have revealed the role of DJ-1 in the anti-oxidative response and established that PINK1 and Parkin act in the same pathway to control mitochondrial physiology (Bier, 2006). These results point to a distinct molecular pathway involved in the demise of dopaminergic neurons in PD.
In order to efficiently respond to hazardous conditions, cellular ROS sensors exist that monitor oxidative stress and regulate either the expression of antioxidant genes or genes that promote cell death (Storz, 2006). The nucleolus, traditionally regarded as the organelle of ribosome biosynthesis, has recently been implicated in sensing and responding to cellular stress by stabilizing the protein 53 (p53) (Rubbi and Milner, 2003, Mayer and Grummt, 2005, Boisvert, et al., 2007, Kruhlak, et al., 2007).

2.6 The nucleolus: site of ribosomal RNA synthesis

The nucleolus is a distinct sub-nuclear compartment that was first observed more than 200 years ago. It is roughly spherical and surrounded by a layer of condensed chromatin. Nucleoli assemble around the tandemly repeated ribosomal DNA gene clusters and 28S, 18S and 5.8S ribosomal RNAs (rRNAs) are transcribed as a single precursor (pre-RNA). Subsequently the precursors are processed and assembled with the 5S rRNA into ribosome subunits (Boisvert, et al., 2007). Although the nucleolus is primarily associated with ribosome biogenesis, several lines of evidence show that it has additional functions, like regulation of mitosis, cell-cycle progression, proliferation, and more recently many forms of stress response (Olson, et al., 2002).

Mammalian cells contain 100 or more copies of tandemly repeated rRNA genes per haploid genome. These genes are transcribed with high efficiency to keep up with the cells metabolic activity and demand for ribosomes. Alterations in cell proliferation are accompanied by profound changes in the transcription rate of rRNA genes by RNA polymerase I (Pol I), responsible for the transcription of large rRNA genes. Thus, by responding to changes in the cellular environment, transcription by Pol I ultimately determines ribosome production and the potential for cell growth and proliferation or survival (Boisvert, et al., 2007).

2.7 RNA polymerase I

RNA polymerase I (Pol I) is a multimeric protein complex and its sole function is the transcription of genes encoding the large rRNAs (28S, 18S and 5,8S). Like RNA polymerase II and III it requires auxiliary factors that mediate promoter recognition, promote transcription elongation and facilitate transcription termination. RNA polymerase I needs at least four basal transcription initiation factors, upstream binding factor (UBF), the promoter selectively factors transcription initiation factor-IA (TIF-IA), transcription initiation factor-IB (TIF-IB) and transcription initiation factor-IC (TIF-IC) (Fig.

3). The key player in growth-dependent regulation of rDNA transcription is TIF-IA. A pre-initiation complex containing Pol I can be formed in the absence of TIF-IA, however formation of the first phosphodiester-bond of the RNA transcript requires the presence of TIF-IA. Following initiation, TIF-IA is released from the ternary complex and can associate with another pre-initiation complex. The activity of TIF-IA is regulated by diverse extracellular signals, suggesting that this factor adapts Pol I transcription to cell growth (Schnapp, et al., 1990, Yamamoto, et al., 1996, Bodem, et al., 2000, Mayer and Grummt, 2005).

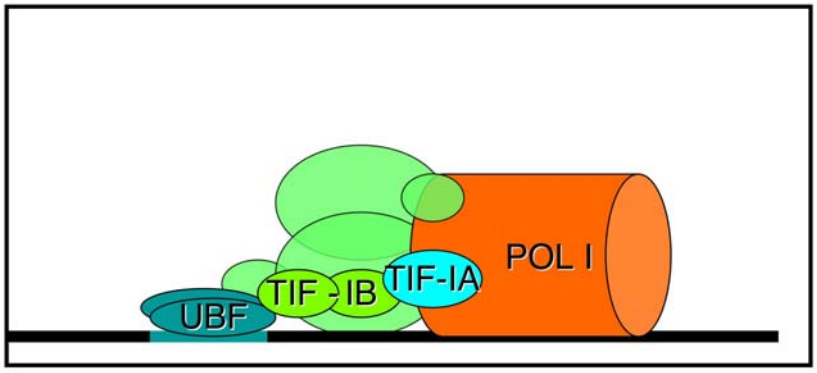

Figure 3: Scheme of the recruitment of the RNA polymerase I (Pol I) to the rDNA sequences.
Dimers of the upstream binding factor (UBF) bind to the UBE. A pre-initiation complex is formed by binding to various transcription initiation factors, like TIF-IA and TIF-IB. Recruitment of RNA Polymerase I to that complex concludes the formation of a transcriptional complex.

2.8 Transcription initiation factor I A (TIF-IA)

TIF-IA was initially identified as 'an activity' that complements transcriptional inactive extracts obtained from quiescent mouse cells (Buttgereit, et al., 1985). Interactions between TIF-IA with Pol I are affected by diverse regulatory pathways that link the cells biosynthetic activities to environmental conditions. For example, it has been shown that nutrients starvation, density areas and protein synthesis inhibitor lead to inactivation of TIF-IA

(Cavanaugh, et al., 2002, Yuan, et al., 2005). Another mode of transcriptional regulation is phosphorylation. Since TIF-IA possesses multiple phosphorylation sites. It was shown that signals affecting cell metabolism alter the phosphorylation pattern of TIF-IA, for example in density arrested, cycloheximide treated and amino-acid starved cells TIF-IA is hypophosphorylated and incapable of binding Pol I. (Zhao, et al., 2003). The importance of this particular factor became clear with the reports that inactivation of the TIF-IA gene (knockout) in mice resulted in prenatal lethality. In addition in mouse embryonic fibroblasts (MEFs) Cre-mediated depletion of TIF-IA leads to disruption of nucleoli, cell cycle arrest, upregulation of p53 and induction of apoptosis (Yuan, et al., 2005, Grewal, et al., 2007).

Under normal conditions, murine double minute 2 protein (MDM2) maintains p53 at low levels through ubiquitination and degradation by proteasomes (Tao and Levine, 1999, Sugimoto, et al., 2003). Under a variety of stress conditions certain ribosomal proteins (Lohrum, et al., 2003) or proteins associated with preribosomes, such as nucleophosmin (NPM, B23)(Kurki, et al., 2004) interact with MDM2 protecting p53 from degradation. These findings indicate that nucleolar proteins may trigger cellular damage responses by interfering with p53 turnover (Vousden and Lane, 2007).

The correlation between perturbation of nucleolar function, elevated levels of p53 and induction of cell suicide supports the view that the nucleolus is a stress sensor and regulates p53 activity (Yuan, et al., 2005). So far there is no evidence that link the nucleolar function and oxidative stress in dopaminergic neurons.

2.9 Aim of this thesis

Oxidative stress seems to be the major cause for the demise of dopaminergic neurons and therefore is one of the suspects intensively investigated among others that cause and/or promote PD. Aim of the present study was the analysis of the importance of the nucleolus in the oxidative stress response in dopaminergic neurons and its implications in the etiology of PD.

Therefore the ability of the nucleolus to react upon oxidative stress in dopaminergic neurons was evaluated. Monitoring nucleolar integrity and activity should reveal a mutual relationship between oxidative stress and nucleolar perturbation. To further evaluate the role of the nucleolus, mouse mutants in which the nucleolus is artificially disrupted by the ablation of TIF-IA in dopaminergic neurons were generated using the Cre/loxP recombination system. The additional generation of an inducible Cre-recombinase mouse line allowed a spatio-temporal regulation of nucleolar disruption and thereby enabling to analyze the sequence of events, happening upon nucleolar disruption in dopaminergic neurons, more precisely.

The analysis was concluded by the examination of human cases of PD in order to determine the involvement of the nucleolus (and rDNA transcription) in the development and progression of PD.

3. Results:

3.1 MPTP affects nucleolar integrity and function.

The nucleolus has recently been implicated in sensing of and responding to cellular stress (Olson, et al., 2002, Rubbi and Milner, 2003, Michel, et al., 2006). To test if the nucleolus possesses the ability to react upon oxidative stress in dopaminergic neurons, nucleolar integrity and activity was monitored after injection of MPTP, a selective dopaminergic neurotoxin that inhibits the mitochondrial respiratory chain, leading to impaired energy production and increased oxidative stress (Przedborski and Vila, 2003, Schober, 2004).

In control mice, the nucleoli within dopaminergic neurons are clearly visible as distinct punctuate nucleolar structures as revealed by nucleophosmin (NPM) distribution (Fig. 4a). After treatment with MPTP, nucleolar structure starts to be perturbed and NPM is found throughout the nucleoplasm (Fig. 4b,c). In situ hybridization using a digoxygenin-labeled probe against the 5'-ETS (externally transcribed spacer) of pre-rRNA revealed a strong reduction of nucleolar transcriptional activity in the midbrain of mice treated with MPTP (Fig. 4e) compared to mice treated with physiological saline (Fig. 4d). No significant change of pre-rRNA synthesis was observed in areas of the brain that are not targeted by the toxin, e.g. the hippocampus (Fig. 4f,g). Quantification of the in situ hybridization signals in tyrosine hydroxylase (TH^+) containing dopaminergic neurons revealed that one day after MPTP administration the synthesis of pre-rRNA is already decreased by ~50% (Fig. 4h).

The finding that MPTP treatment not only impaired mitochondrial function in dopaminergic neurons but also affected the structure and transcriptional activity of nucleoli, suggests a link between nucleolar and mitochondrial function in MPTP-induced parkinsonism.

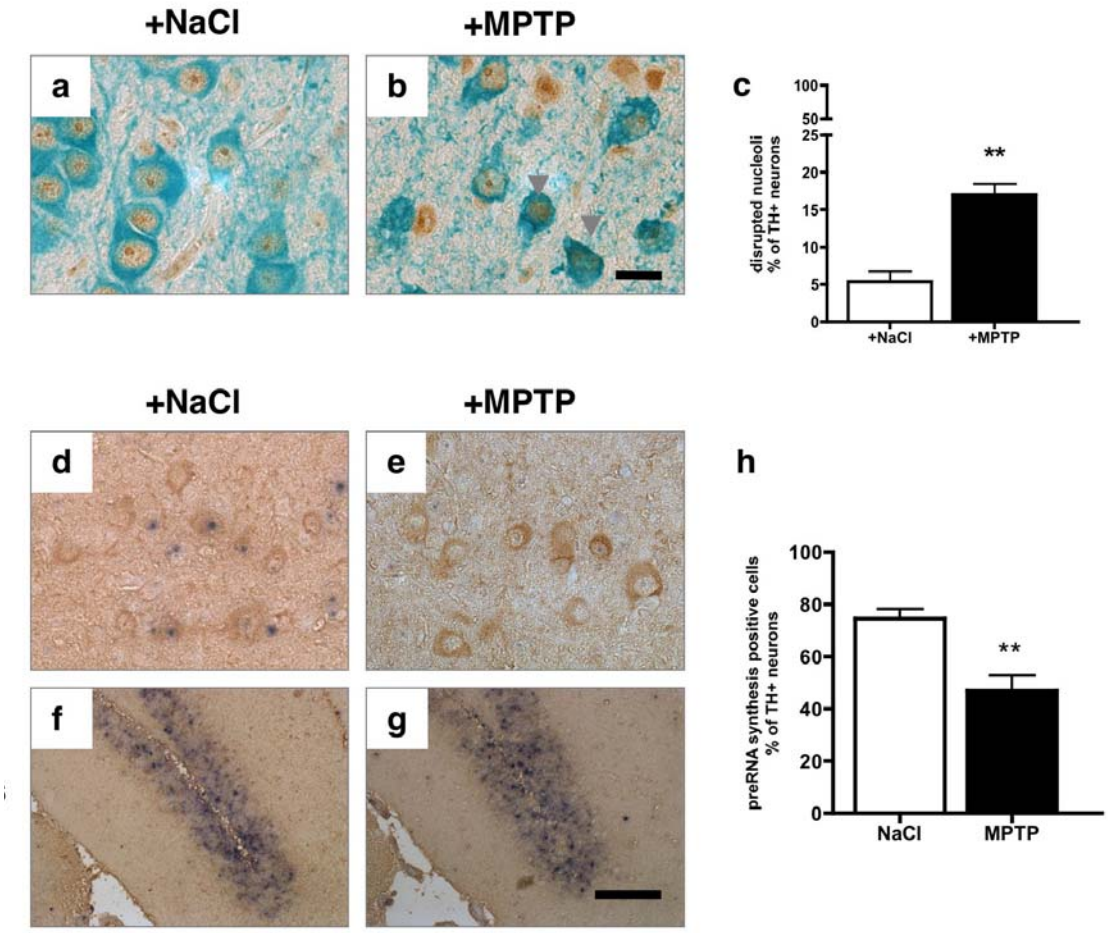

Figure 4: **Effect of MPTP treatment on nucleolar activities.**
(**a,b**) Detection of nucleolar integrity in dopaminergic neurons by immunohistochemistry using NPM (brown) and TH (green) antibodies in 2 months old mice injected with either MPTP or saline over 3 days and analyzed 1 day after the last MPTP injection. (**c**) Quantification of the nucleolar disruption in dopaminergic neurons of mice injected with MPTP or saline by counting TH+ neurons showing NPM nuclear translocation (n=5; **, p<0.01). (**d-g**) Effect of MPTP on 47S pre-rRNA synthesis in the midbrain (**d,e**) and hippocampus (**f,g**) of mice treated with NaCl (**d,f**) or with MPTP (**e,g**). In situ hybridizations using a riboprobe recognizing the 5´ETS of the 47S pre-rRNA (blue) and TH immunohistochemistry (brown) to identify dopaminergic neurons are shown. (**h**) Quantitative analysis of pre-rRNA signals, expressed as number of blue dots in dopaminergic neurons in mice treated with NaCl and MPTP, shows reduced pre-rRNA levels in MPTP treated mice (n=3; **, p<0.01). Scale bars: b, 15µm; g, 100µm.

3.2 Progressive loss of dopaminergic neurons by genetic ablation of TIF-IA.

The decrease in Pol I transcription after MPTP-induced oxidative stress revealed a functional interrelationship between the nucleolus and mitochondria. To explore the consequence of perturbing this interrelationship nucleolar function was specifically ablated in dopaminergic neurons by Cre-mediated excision (Fig. 5) of the essential Pol I-specific loxP flanked exon of transcription factor TIF-IA allele (TIF-IA^{fl}), which has been shown to cause nucleolar perturbation (Yuan, et al., 2005). TIF-IA$^{fl/fl}$ mice were crossed with mice expressing the Cre recombinase under the control of the regulatory elements of the dopamine transporter gene (DATCre)(Parlato, et al., 2006).

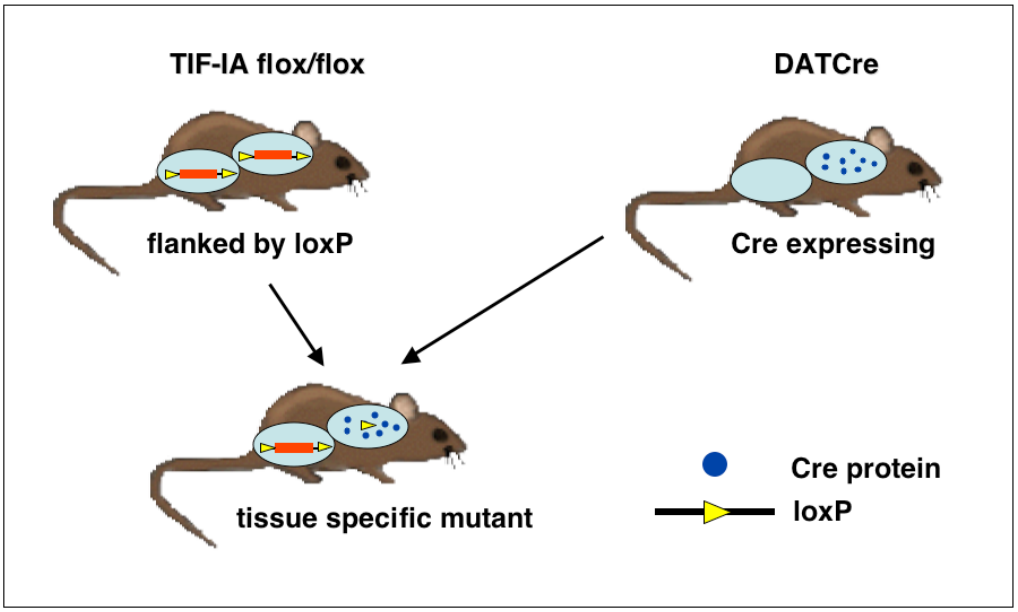

Figure 5: The Cre/loxP recombination system allows cell-type specific inactivation of a target gene
To achieve cell-type specific gene inactivation using the Cre/loxP-recombination system, an essential part of a gene has to be flanked by loxP sequences, without affecting the expression of the gene. The cell-type/tissue-specific expression of the Cre recombinase under control of specific regulatory elements results in deletion of the part that is flanked and thereby the gene inactivation occurs exclusively in Cre-expressing cells.

Until day 15, TIF-IAfl/fl; DATCre mutants (TIF-IA^{DATCre}) were indistinguishable from control littermates. Thereafter, they were smaller and weighed less and these differences progressed with age (Fig. 6a).

After 4 weeks TIF-IA^{DATCre} mutants exhibited motor impairment, starting with slowness of movements, gait and posture disturbances and resting tremor resembling PD symptomatology. These locomotor abnormalities were associated with alterations in the number of dopaminergic neurons. At P0, the number of neurons, identified by immunohistochemistry (IHC) with TH antibodies, was similar in control and TIF-IA^{DATCre} mice, while at later stages dopaminergic neurons were progressively lost (Fig. 6b,c). Importantly, dopaminergic neurons in the substantia nigra (SN) (Fig. 6b) were more rapidly and strongly affected than those in the ventral tegmental area (VTA) (Fig. 6c), mimicking the differential vulnerability of these two subpopulations of dopaminergic neurons in PD.

To prove that dopaminergic neurons are preferentially lost in the SN the expression of TH (Fig. 6d,e), Cre recombinase (Fig. 6f,g) and p53 was monitored by immunohistochemical analysis (Fig. 6h,i). The dopaminergic neurons in the VTA also showed strong p53 upregulation (Fig. 6h,i), indicating that these neurons are less sensitive to the consequences of nucleolar perturbation.

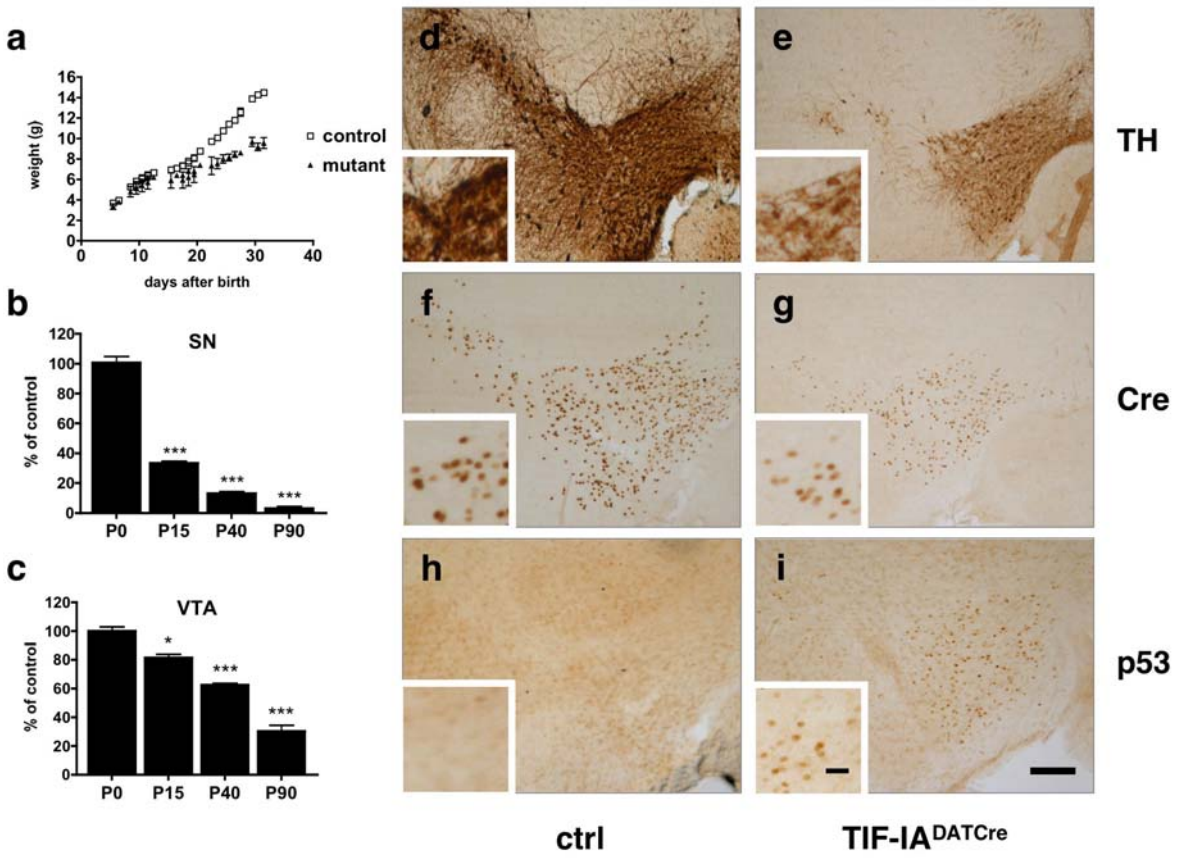

Figure 6: Progressive loss of dopaminergic neurons in TIF-IA^{DATCre} mutant mice. (**a**) Weight curves show growth differences between control and TIF-IA^{DATCre} littermates starting at P15 (n=8). (**b,c**) Quantification of TH^{+} neurons at different postnatal stages (P0, P15, P40, P90) revealed that mutant and control mice did not show any significant differences in number of dopaminergic neurons at birth, whereas they are progressively lost at later stages. Substantia nigra (SN) neurons (**b**) are more susceptible to the loss of TIF-IA than ventral tegmental area (VTA) neurons (**c**) (n=5). (**d-g**) Immunohistochemistry with antibodies specific for TH (D,E) or Cre recombinase (**f,g**) shows the preferential loss of dopaminergic neurons within the SN in mutant mice (**e,g**) compared to control mice (**d,f**) at P30. A littermate mouse expressing the Cre is shown as control. (**h,i**) Remaining dopaminergic neurons in the mutant VTA show p53 overexpression (**i**) whereas p53 level in control mice appear undetectable (**h**). (*, p<0.05; **, p<0.01; ***, p<0.001). Scale bar: 100μm, insert 50μm.

3.3 Loss of striatal dopamine in TIF-IA^{DATCre} mutants.

Loss of dopaminergic neurons in PD patients impairs dopamine production, leading to alterations of the neural circuits that regulate movement (Lang and Lozano, 1998b). Likewise, TIF-IA^{DATCre} mutants show locomotor abnormalities and progressive loss of dopaminergic neurons in the ventral midbrain. At P7, i.e. before dopaminergic neurons were lost, TH immunoreactivity in the striatum in TIF-IA^{DATCre} mice was reduced (Fig. 7b) and was barely detectable at P15 (Fig. 7d). Moreover, there was a gradual loss of TH-staining intensities in striata of mutant mice (Fig. 7e). The expression of the dopamine D1 receptor in dopaminoceptive neurons did not change in TIF-IA^{DATCre} mutants, which underscores the specificity of the targeted mutational approach (Fig. 7 f-h). Therefore, the observed phenotype recapitulates the selective loss of SN neurons observed in PD.

To test whether loss of dopaminergic neurons should decrease the striatal dopamine content, we analyzed dopamine levels by High Performance Liquid Chromatography (HPLC) and electrochemical detection. TIF-IA^{DATCre} mice showed a 95% reduction of dopamine levels at 5 weeks of age compared to control mice (n=5) (Fig. 8a).

The reduced striatal dopamine transmission should lead to impaired locomotor activity in TIF-IA^{DATCre} mutants compared to control mice of the same age. To assess locomotor dysfunction, the accelerating rotarod assay was performed, recording the time spent by the mice on the accelerating wheel (Yoshida, et al., 2003). At 4 weeks of age, a ~50% reduction in motor performance of mutant mice was observed compared to controls. This decrease reached a ~65% decline at 8 weeks of age (Fig. 8b). Together, these results demonstrate that ablation of TIF-IA leads to progressive loss of dopaminergic neurons in the SN and VTA, reduction of the striatal dopamine content and severely impaired locomotor performance.

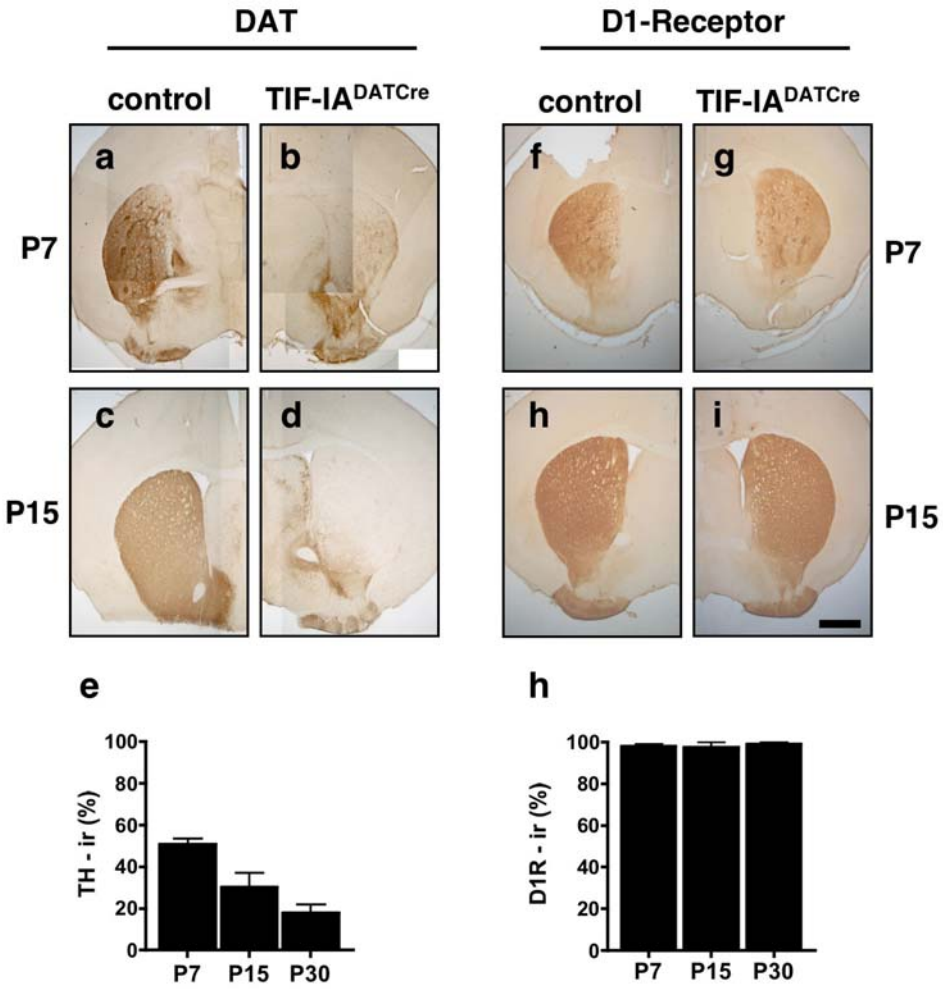

Figure 7: TIF-IA^{DATCre} mutants show progressive loss of TH immnoreactivity in striata.
(**a-d**) Immunohistochemistry specific for TH performed at P7 and P15 in control (**a,b**) and TIF-IA^{DATCre} mutants (**c,d**).(**e**) Levels of TH immunoreactivity (TH-ir) in striata at P7, P15 and P30 were normalized to control littermates and plotted as a histogram (n=4) for each time point. (**f-h**) No effect on dopaminoceptive neurons in TIF-IA^{DATCre} mutants. Postsynaptic cells in the striatum visualized by dopamine D1 receptor immunohistochemistry on sections of TIF-IA^{DATCre} (**g,i**) and control mice (**f,h**) at different stages (P7, P30) remained unchanged. No differences are visible between mutants (**g,f**) and respective controls (**f,h**) at P7, P15 and P30. (**h**) Levels of D1 receptor immunoreactivity (D1R-ir) in striata at P7, P15 and P30 were normalized to control littermates and plotted as a histogram (n=4) for each time point. Scale bar: 250µm.

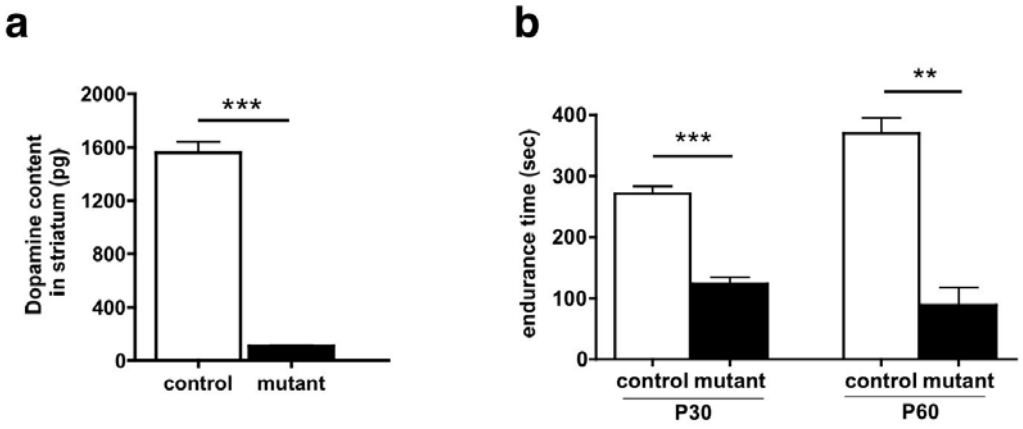

Figure 8: Lack of striatal dopamine leads to impaired locomotor activity
(**a**) At P40 the dopamine content in striata measured by HPLC-ED showed a 95% reduction in comparison to the control group (n=5). (**b**) Locomotor deficits of TIF-IA^{DATCre} mice determined by the accelerating rotarod assay. At P30 mutants showed a locomotor deficit of 55% and at P60 of 76% compared to control mice (n=5; p<0,01; ***, p<0,001).

3.4 Rescue of TIF-IA^{DATCre} mutant mice by L-DOPA treatment.

Given that the main neuropathological feature of PD is the progressive demise of dopaminergic neurons, therapies for PD enhancing synaptic dopamine transmission have been developed. Among these, the dopamine precursor L-3,4-dihydroxyphenylalanine (L-DOPA) still occupies a preeminent place (Carlsson, et al., 1957, Birkmayer and Hornykiewicz, 1961). We asked whether this treatment for PD symptomatology would rescue TIF-IA^{DATCre} mutant mice from developing the symptoms described above and from death. To this end, L-DOPA (50mg/kg) was injected daily over 3 weeks in 7 weeks old mice that already show a rather severe phenotype (n=4). While mutants without treatment with L-DOPA did not gain weight and died early, mutant mice treated with L-DOPA gained weight, showed reduced behavior abnormalities and were rescued from death (Fig. 9a). Moreover, increased growth of TIF-IA^{DATCre} mice was achieved 6 weeks after continuous treatment by implanting subcutaneous pellets releasing a constant amount of L-DOPA (Fig. 9b). Together, these data demonstrate the responsiveness of TIF-IA^{DATCre} mutants towards L-DOPA administration, recapitulating an important characteristic of PD.

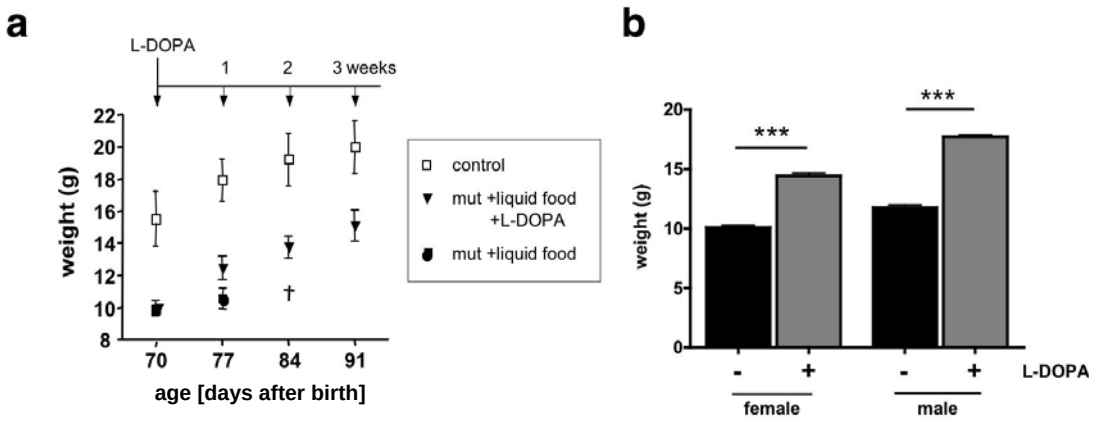

Figure 9: L-DOPA administration increases lifespan of TIF-IA^{DATCre} mice
(**a**) Rescue of TIF-IA^{DATCre} mice by L-DOPA injection. Mutant mice (7 weeks-old) treated by daily injecting L-DOPA for 3 weeks gained weight similarly to control mice, while untreated mutant mice died without gaining weight despite supplementation with liquid food (n=4). (**b**) Longer treatment (60 days) was achieved by implantation of a pellet releasing a constant amount of L-DOPA subcutaneously. Mutants display weight gain independent of sex (n=5; ***, p<0.001).

3.5 Reduced mitochondrial activity upon nucleolar impairment

Given the crucial role of mitochondrial dysfunction in PD, most strikingly reflected in patients with mutations in DJ-1, PINK1, Parkin and in Drosophila mutants modeling the disease (Vila and Przedborski, 2003, Moore, et al., 2005, Abou-Sleiman, et al., 2006, Lin and Beal, 2006, Moore, et al., 2006), we assessed whether interference with TIF-IA activity and nucleolar integrity will lead to impaired mitochondrial function. TIF-IA^{DATCre} embryos at E18.5 were used and nucleolar expression of TH as a marker for dopaminergic neurons, Cre as a marker for expression of the transgene and p53 serving as a marker for nucleolar perturbation upon TIF-IA loss were monitored. At E15.5 only a few dopaminergic neurons express a detectable amount of Cre recombinase (Fig. 10b) and display p53 upregulation (Fig. 10c). In embryos at E18.5 Cre recombinase was detectable (Fig. 10h) and almost all dopaminergic neurons display p53 upregulation (Fig. 10i) suggesting that loss of TIF-IA occurred.

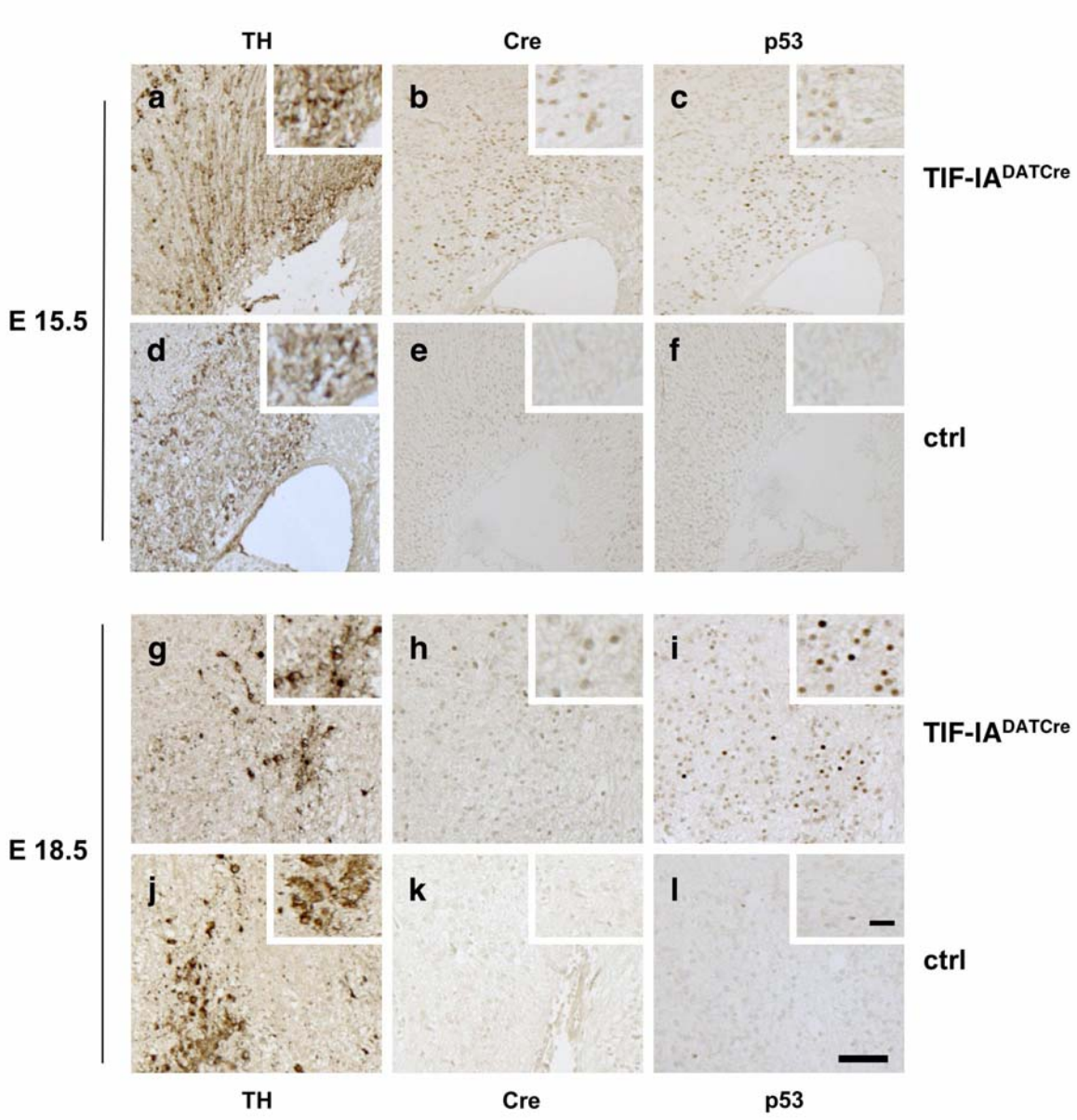

Figure 10: Response of dopaminergic neurons to TIF-IA ablation during embryonic development.
(**a-f**) Adjacent sagittal sections of control and TIF-IA^{DATCre} mutants at E15.5 stained with antibodies against TH, Cre and p53. (**a,d**) TH is used for the identification of dopaminergic neurons in the ventral mesencephalon. (**b,e**) Expression of Cre-recombinase in the same area (**b**) associated with p53-overexpression in the TIF-IA^{DATCre} mutants (**c**), but not in control (**e,f**). (**g-l**) At E18.5 more cells are affected by the mutation in comparison to control (**j-l**), as visualized by the overexpression of p53 in the mutants (**i**). Scale bar 50µm, inserts 20µm.

One of the most frequent causes of mitochondrial defects is reduced activity of the cytochrome c oxidase (COX), and so COX activity is used as a marker for impaired mitochondrial activity (Bender, et al., 2006, Ekstrand, et al., 2007). Embryos at E18.5, where TIF-IA ablation clearly affected most dopaminergic neurons were analyzed. In control embryos NPM is localized within the nucleoli, whereas in TIF-IA^{DATCre} mutants NPM is distributed throughout the nucleoplasm (Fig. 11a,b) as a result of TIF-IA loss. The nucleolar perturbation is accompanied by strong reduction of COX activity in the ventral mesencephalic area (Fig. 11d) compared to control mice (Fig. 11c), indicating that loss of TIF-IA function affects mitochondrial activity.

Intriguingly, nucleolar disruption influences mitochondrial activity before structural changes in dopaminergic neurons or their projections to the striatum became visible.

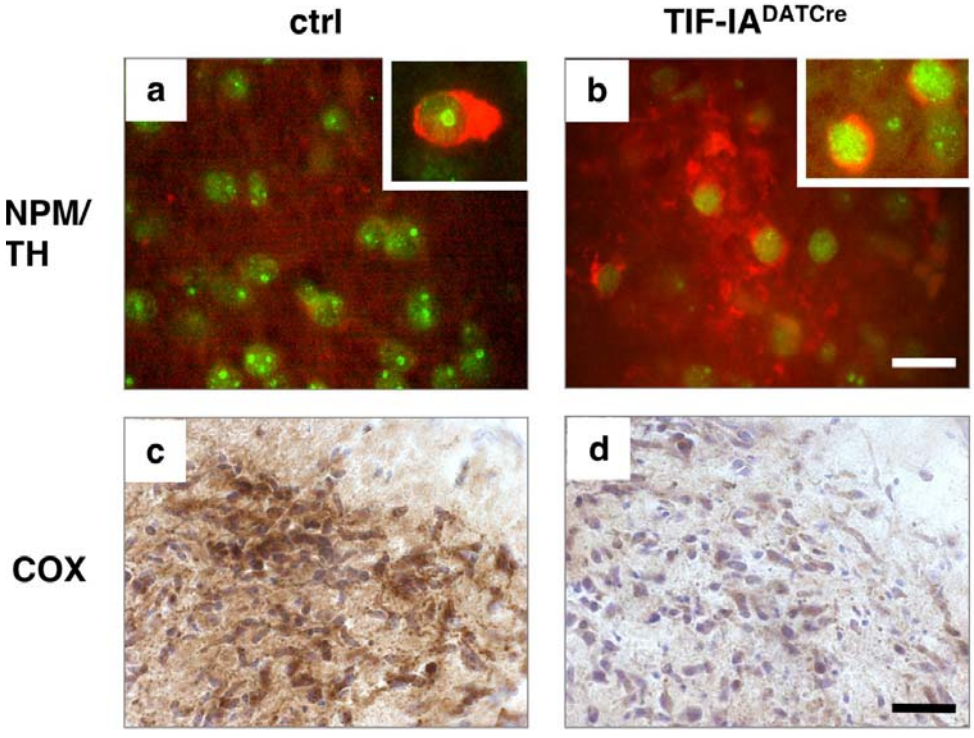

Figure 11: Mitochondrial impairment upon nucleolar disruption.
(**a,b**) Double immunoflorescence with NPM/B23 (green) and TH (red) shows disruption of nucleoli in TIF-IA^{DATCre} mutants at E18.5 in dopaminergic neurons, while nucleoli of control mice appear normal. (**c,d**) Control mice display intact COX activity (brown), whereas in TIF-IA^{DATCre} mice respiratory chain deficient neurons show violet cytoplasmic staining due to lack of COX activity. Scale bars: a,b, 20μm; c,d, 75μm.

3.6 Generation of a mouse line expressing an inducible Cre-recombinase exclusively in dopaminergic neurons

In order to assess in more detail the sequence of events that link nucleolar with mitochondrial function and to avoid developmental defects due to TIF-IA depletion during embryogenesis, we intended to generate transgenic mice expressing an inducible Cre recombinase in dopaminergic neurons. To achieve inducible recombination of conditional alleles in dopaminergic neurons of the adult brain, a BAC-derived transgene expressing the CreER^{T2} fusion protein under the control of the regulatory elements of the mouse DAT gene (DATCreER^{T2}) was generated. The CreER^{T2} fusion protein consists of the Cre recombinase and a mutated ligand-binding domain (LBD) of the human estrogen receptor (ER) (Feil, et al., 1997, Indra, et al., 1999). The ER-LBD contains a nuclear localization signal that is unmasked upon ligand binding. Two point mutations in the ER-LBD allow activation exclusively by the synthetic ligand tamoxifen. The unliganded form of the CreER^{T2} fusion protein resides in the cytoplasm and only upon tamoxifen binding it translocates into the nucleus and mediates site-specific recombination (Fig. 12).

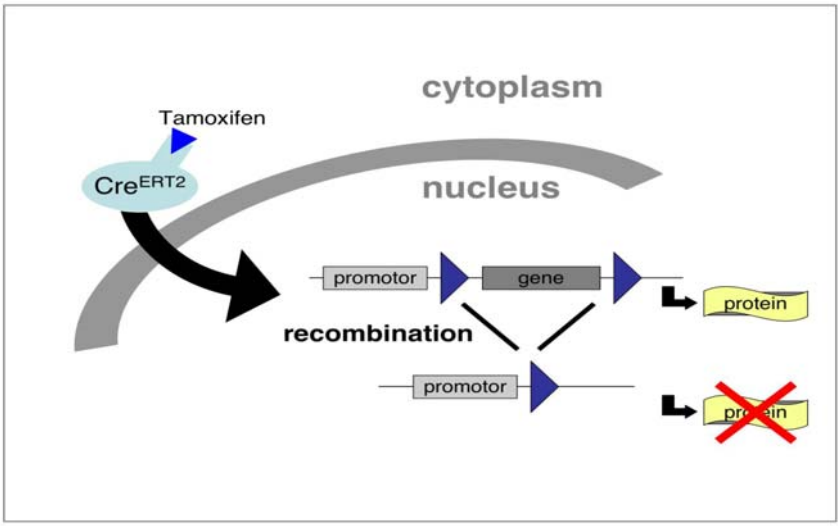

Figure 12: Schema of the inducible Cre/loxP system
The Cre/loxP-recombination system has been modified with the tamoxifen-inducible fusion protein consisting of the Cre recombinase and the mutated ligand binding domain (LBD) of the human estrogen receptor (Cre^{ERT2}) to achieve ligand dependent Cre activity. The unliganded form of the Cre^{ERT2} fusion protein resides in the cytoplasm and upon tamoxifen binding it translocates into the nucleus and mediates site-specific recombination of the loxP-flanked DNA sequence.

A BAC clone was selected that harbored a genomic insert containing the DAT gene locus (42kb) with a 51kb 5'upstream and a 46kb 3'downstream region from the mouse genome project (www.ensembl.org). To obtain the DATCre^{ERT2} transgene, the coding sequence for the CreER^{T2} fusion protein was inserted into the reading frame in the second exon of the DAT locus (Fig. 13) by homologous recombination in bacteria (Lee, et al., 2001). The modified genomic insert was released by NotI digestion and then separated from the BAC backbone and using a gel filtration column. Finally it was introduced into the mouse germline by oocytes injection (Schedl, et al., 1993).

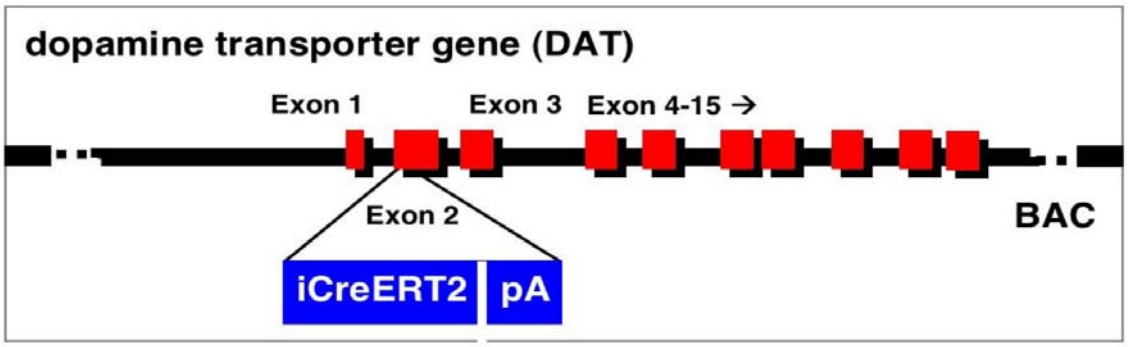

Figure 13: Insertion of the CreERT2 cassette into a genomic BAC clone containing the DAT locus.
The scheme represents the DATCreERT2 BAC construct, showing the position of the inducible Cre gene (iCreERT2), in the second exon in frame at the ATG of the DAT gene.

3.7 Faithfull expression of the CreER^{T2} fusion protein in dopaminergic neurons

Transgenic founder animals were identified by PCR (see material and methods). Two founders containing the transgene were identified and chosen for breeding with C57/Bl6 mice to establish transgenic mouse lines. Two different lines harboring the transgene (called Z1 and Z5) were used. The expression and nuclear translocation of the CreER^{T2} fusion protein upon tamoxifen treatment was investigated by immunohistochemistry (IHC) and immunoflorescence (IF) using midbrain vibratome sections containing SN and VTA. Transgenic animals were injected with either tamoxifen or vehicle

(sunflower oil) 12 hours before dispatch. In vehicle-treated animals the CreER^{T2} protein was located in the cytoplasm (Fig. 14a,b,e,f), whereas tamoxifen-treated animals displayed nuclear localization of the Cre recombinase in SN/ VTA (Fig. 14c,d,g,h).

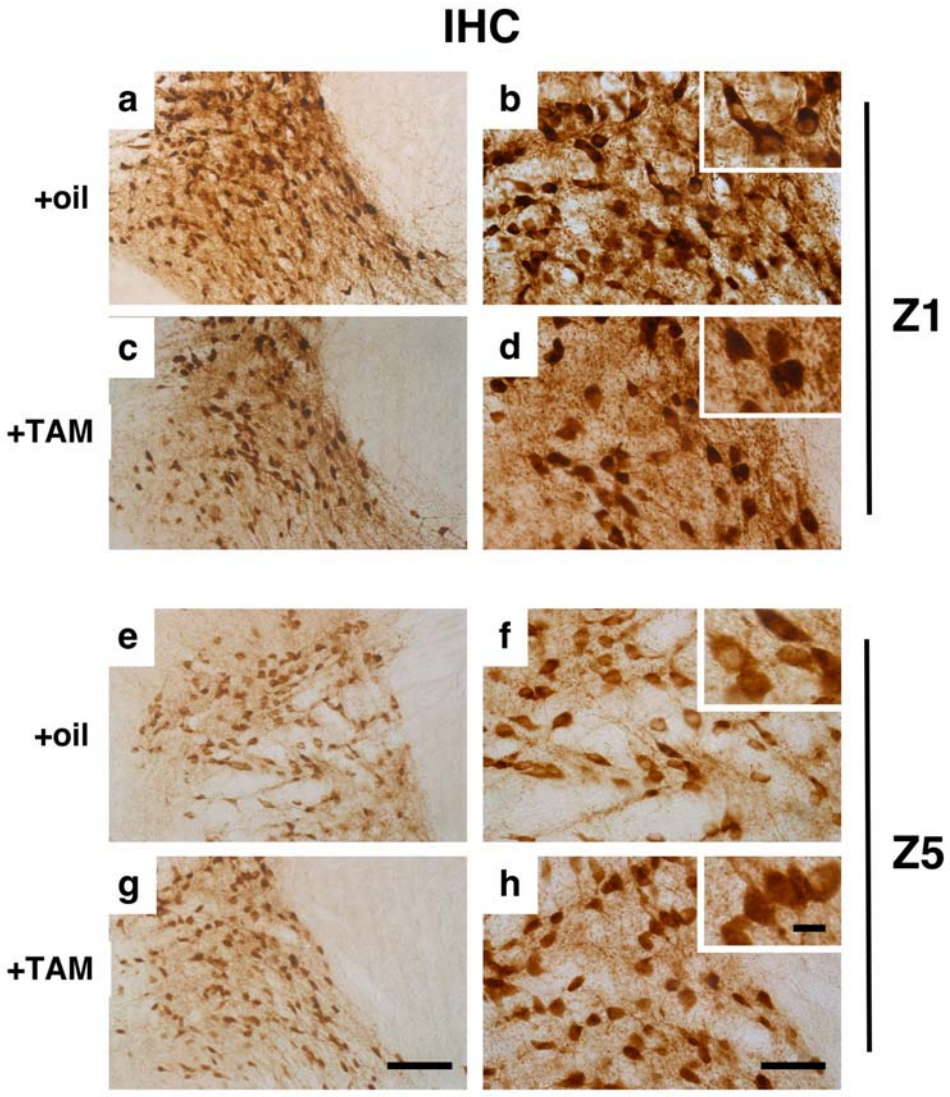

Figure 14: Cre recombinase translocates into the nucleus only upon treatment with Tamoxifen.
Brain sections of two transgenic mouse lines (Z1 and Z5) expressing the inducible Cre recombinase injected either with oil (**a,b,e,f**) or tamoxifen (**c,d,g,h**). Whereas in mice injected with oil the Cre recombinase resides in the cytoplasm, DATCreER^{T2} transgenic mice injected with tamoxifen show nuclear translocation of the Cre recombinase in both transgenic lines Z1 (**c,d**) and Z5 (**g,h**). Scale bar, j, 100 µm; k, 50 µm; inserts, 10µm.

3.8 Targeted tamoxifen-induced recombination in the adult SN/VTA

To assess the ER^{T2}-mediated control of the Cre recombinase activity in the absence of the ligand in dopaminergic neurons and to examine the efficiency of tamoxifen-induced Cre-mediated recombination, the different $DATCreER^{T2}$ mouse lines (Z1 and Z5) were crossed with ROSA26 Cre reporter mice (Soriano, 1999) to obtain ROSA26;$DATCreER^{T2}$ mice. The Cre reporter line harbors a knock-in of the β-galactosidase (lacZ) gene followed by a stop cassette, which is flanked by two recognition sequences for the Cre recombinase (loxP). Upon tamoxifen treatment the Cre recombinase translocates into the nucleus and deletes the stop cassette thereby permitting β-galactosidase expression.

$ROSA26^{DATCreERT2}$ mice were injected twice per day with either tamoxifen (10mg/ml) or vehicle for five consecutive days (Erdmann, et al., 2007). Whole mount samples of the adult brain from the two $DATCreER^{T2}$ lines were analyzed 10 days after the treatment for β-galactosidase activity.

Determination of $CreER^{T2}$ activity in the absence of the ligand revealed that ten weeks old vehicle-injected animals of the two transgenic lines showed very little β-galactosidase activity (Fig. 15a,d,g,i). Using whole mount staining no substantial differences were detected upon tamoxifen treatment between the two different $DATCreER^{T2}$ transgenic lines in the SN/VTA (Fig. 15b,e,h,j).

However, after tamoxifen treatment only the Z1 line shows β-galactosidase activity in dopaminergic neurons in the olfactory bulb and arcuate nucleus (Fig. 15c,f).

Further analyses were carried out using the $DATCreER^{T2}$ line Z1 due to the better expression pattern of the Cre recombinase in dopaminergic neurons. In order to verify that recombination is restricted to dopaminergic neurons co-labeling of LacZ activity (blue) and TH immunoreactivity (brown) (Fig. 16) was performed.

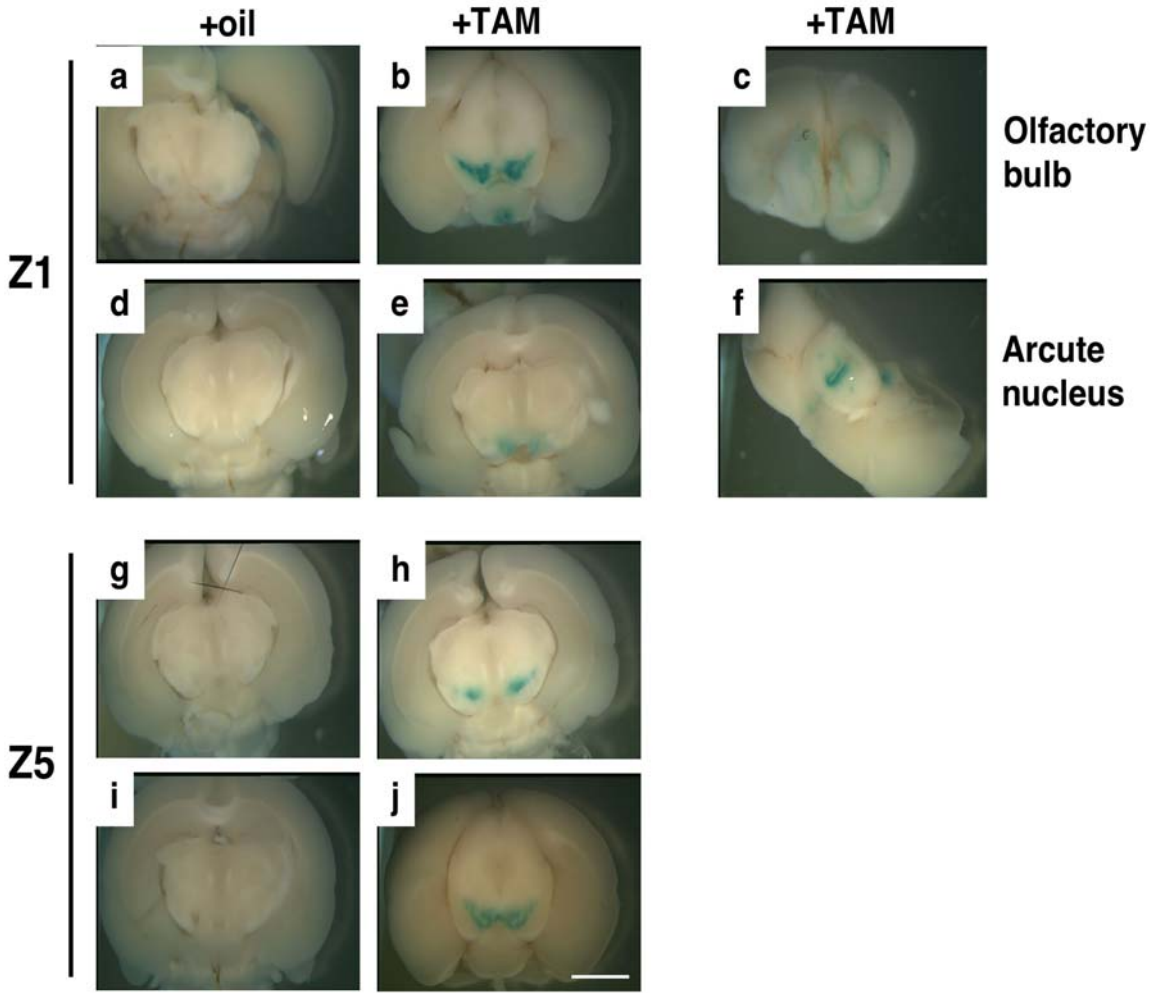

Figure 15: Cre mediated recombination upon tamoxifen treatment
β-galactosidase staining of brain slices from animals harboring a ROSA26 Cre reporter allele and the DATCreER^{T2} transgene. Staining reveals low Cre activity in absence of the ligand only treatment but strong staining within the substantia nigra (**b,e**), ventral tegmental area (**h,j**). In Z1 line (harboring higher number of DATCreER^{T2} transgene) Cre-activity could be additionally observed in the olfactory bulb and arcute nucleus (**c,f**). Scale bar, 400 µm.

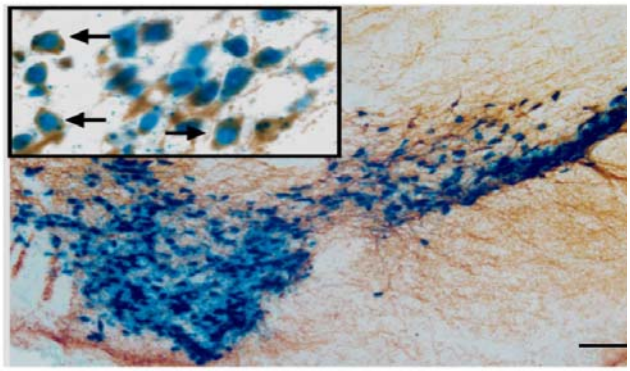

Figure 16: Cre activity is restricted to dopaminergic neurons
The activity of the Cre recombinase is restricted to dopaminergic neurons, as determined by LacZ staining (blue) in combination with TH immunohistochemistry (brown). The insert shows a higher magnification of double-stained neurons (arrows). Scale bar: 125 µm.

3.9 Generation of the inducible TIF-IA^{DATCreERT2} mice

TIF-IA$^{fl/fl}$ mice (Yuan, et al., 2005) were crossed with DATCreER^{T2} mice to generate TIF-IA$^{fl/fl}$; DATCreER^{T2} mice (TIF-IA^{DATCreERT2}), allowed to assess in detail the sequence of events happening after TIF-IA ablation, without developmental impairment.

At the age of 2 months, mutant mice and control littermates were injected twice a day with 1 mg of tamoxifen for five consecutive days (Erdmann, et al., 2007) and sacrificed at 7, 13 and 21 weeks after injection. Immunohistochemical detection of TH was used to analyze the loss of dopaminergic innervations of the striatum (Fig. 17a,c,e,g,i,k) and dopaminergic neurons in the ventral midbrain (Fig. 17b,d,f,h,j,l). After 7 weeks, a significant decrease of TH immunoreactivity was observed in fibers of dopaminergic neurons in the striatum; whereas in the SN this reduction was much less pronounced (Fig. 17b).

13 weeks after induction of Cre recombinase by tamoxifen, loss of TH immunoreactivity in the striatum (Fig. 17g) was associated with a major loss of dopaminergic neurons (Fig. 17h), culminating in an almost complete loss of dopaminergic neurons 21 weeks after induction (Fig. 17l).

Vehicle injected control animals did not show any apparent loss of TH^+ fibers in the striatum (Fig. 17a,c,e) or dopaminergic neurons in the midbrain (Fig. 17a,c,e). TIF-$IA^{DATCreERT2}$ mutants also exhibited a progressive loss of TH^+ fibers in the striatum (Fig. 17g) and dopaminergic neurons in the SN (Fig. 17h) and VTA (Fig. 17i), displaying differential vulnerability of these two subpopulations of dopaminergic neurons upon TIF-IA ablation in the adult.

The quantification of neuronal loss was performed as previously described (Parlato, et al., 2006) and presented for fiber density in the striatum (Fig. 17m), dopaminergic neurons located in the SN (Fig. 17n) and dopaminergic neurons residing in the VTA (Fig. 17o).

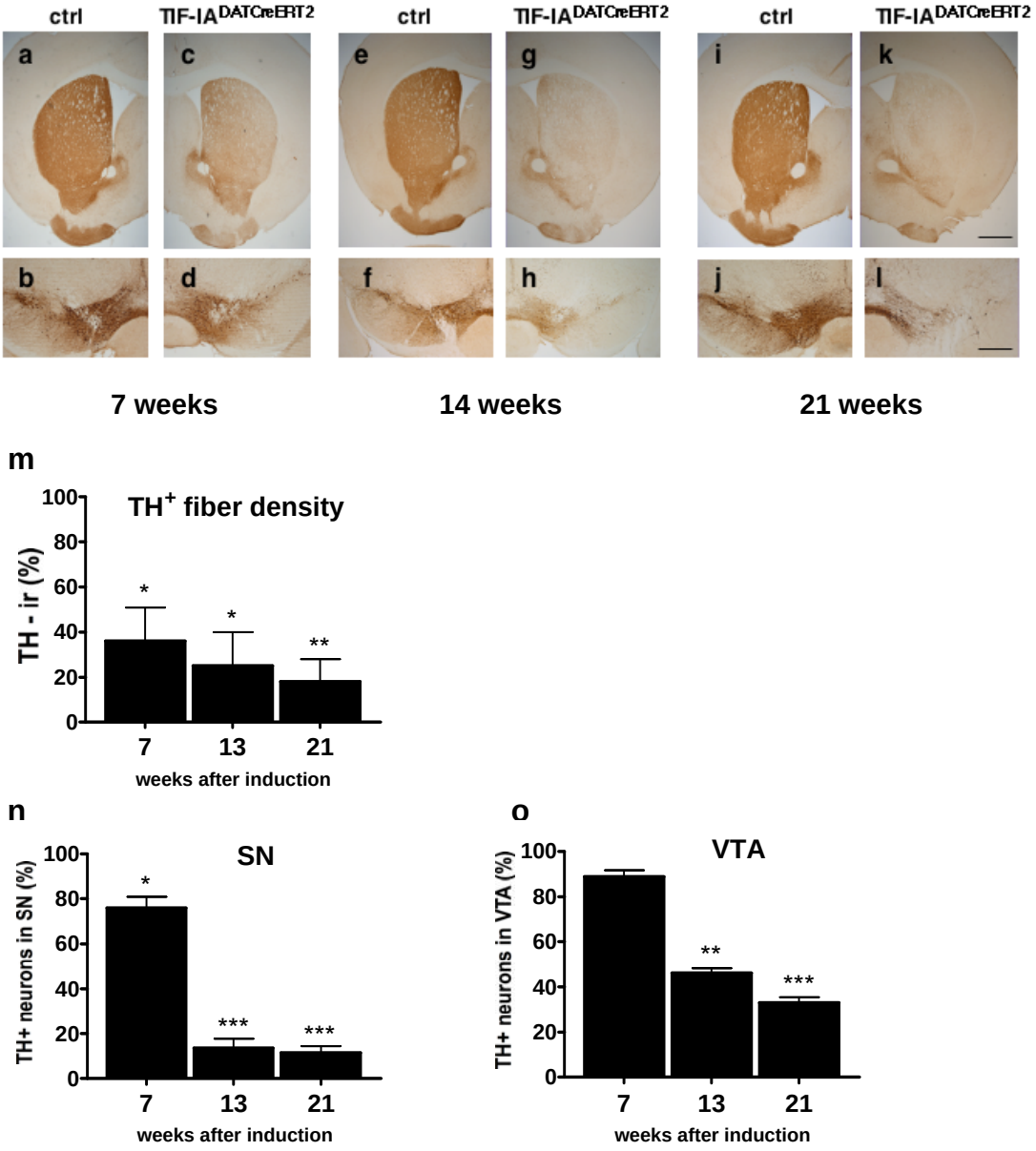

Figure 17: Progressive loss of dopaminergic neurons in TIF-IA^{DATCreERT2} adult mice.
(**a-l**) Loss of TH immunoreactivity in striata is visible in TIF-IA^{DATCreERT2} mutants (**c,d**) 7 weeks after tamoxifen injection compared to control (**a,b**), while TH$^+$ neurons in SN/VTA are minimally affected. 13 weeks after injection, TH$^+$ fibers in striata disappear almost completely (**g**) and severe loss of dopaminergic neurons in SN (**h**) is visible accompanied by partial loss of VTA TH$^+$ neurons. Loss of dopaminergic fibers and neurons further advances 21 weeks after induction with tamoxifen (**k,l**). No changes are visible in the respective controls at 7, 13 and 21 weeks (**a,b**), (**e,f**) and (**i,j**). (**m**) Quantification of the TH$^+$ immunoreactivity in TIF-IA^{DATCreERT2} mice in the striatum compared to respective control mice (n=5). (**n,o**) Percentage of remaining dopaminergic neurons in SN and VTA of mutants in comparison to control littermates (n=4; *, p<0.05; **, p<0.01; ***, p<0.001). Scale bars: k, 200 µm; l, 75µm.

As a next step locomotor activity of TIF-IA^{DATCreERT2} mutants was monitored at different time points (8, 16 and 30 weeks) after tamoxifen-induced Cre expression. After 8 weeks, mutant and control mice did not exhibit significant differences in endurance time on accelerating wheel of the rotarod, consistent with the minor loss of dopaminergic neurons (~20%) at this time (Fig. 18). At 16 weeks, however, a progressive decrease in endurance time was observed, reflecting the decreased number of dopaminergic neurons after Cre-mediated TIF-IA ablation. In addition mutant mice display similar phenotypes as observed with the constitutive mutants (bradykinesia, rigidity, tremor). Taken together, these results demonstrate that progressive loss of dopaminergic neurons in adult TIF-IA^{DATCreERT2} mice leads to decreased locomotor activity and symptoms strikingly similar to those of observed in TIF-IA^{DATCre} mice and in Parkinson's disease patients (Schober, 2004).

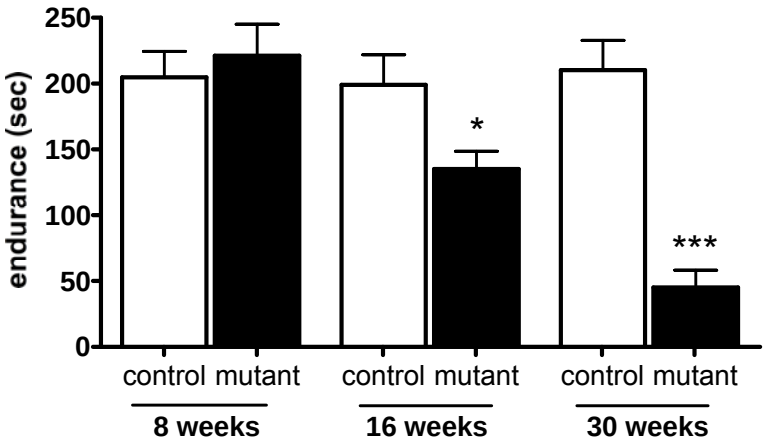

Figure 18: Loss of dopaminergic neurons in TIF-IA^{DATCreERT2} adult mice results in progressive locomotor deficits.
Locomotor deficits of TIF-IA^{DATCre} mice determined by the accelerating rotarod. No differences in motor performance are detectable 8 weeks after tamoxifen injection. 16 weeks after injection the TIF-IA^{DATCreERT2} mutants display a 35% reduction compared to the control group, reaching 75% reduction after 30 weeks. (n≥4; (*, p<0.05; ***, p<0.001).

3.10 Progressive loss of dopaminergic neurons is occasionally accompanied with Lewy body formation

On the cellular level, PD is characterized by the occasional formation of cytoplasmatic proteinaceous inclusion bodies called Lewy bodies, consisting of parkin, synphilin, alpha-synuclein and ubiquitin. Since TIF-IA^{DATCreERT2} mice display progressive loss of neurons finally leading to motor impairment, it was interesting to see whether the mutation also induced the formation of Lewy bodies. Therefore mice were analyzed for specific markers of Lewy bodies 30 weeks after tamoxifen injection. In comparison to control littermates expression of parkin (Fig. 19b) and synphilin (Fig. 19d) was increased, while ubiquitin (Fig. 19f) remained unchanged. Sporadically, immunohistochemical analysis showed neurons with α-synuclein accumulation in mutants (Fig. 19h). These inclusions could also be detected by hematoxylin and eosin (H&E) staining (Fig. 19j).

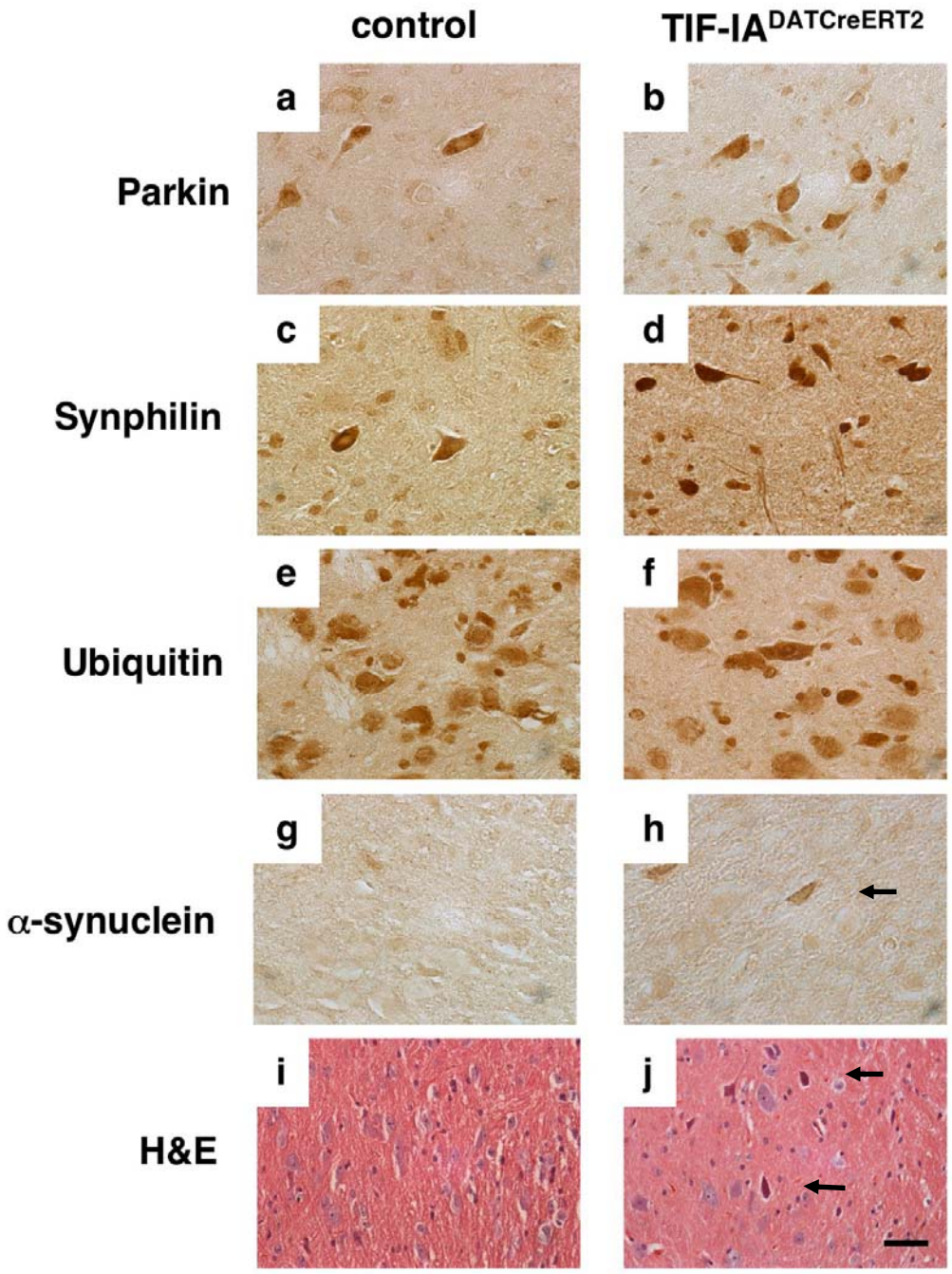

Figure 19: Increased expression of proteins associated with Lewy body formation.
(**a-j**) Brain sections through the ventral midbrain were analyzed for parkin (**a,b**), synphilin (**c,d**), ubiquitin (**e,f**), α-synuclein (**g,h**) and hematoxylin/eosin (H&E) (**i,j**), as markers for Lewy body formation. While parkin and synphilin show higher expression in mutant mice, expression of ubiquitin and H&E are unchanged. Some inclusions could be observed which showed α-synuclein immunoreactivity. Scale bar: a-j, 25 µm

3.11 Linking nucleolar activity and mitochondrial integrity

The results obtained with the inducible TIF-IA^{DATCreERT2} mice encouraged us to assess in more detail the sequence of events that link nucleolar structure degeneration. TIF-IA^{DATCreERT2} mice and control littermates were examined 1, 2 and 4 weeks after tamoxifen injection, i.e. at times when no loss of DA neurons takes place. After 2 and 4 weeks there was a dramatic increase in the number of disrupted nucleoli in TH$^+$ neurons of mutant mice (Fig. 20a). Again, nucleolar disruption was accompanied by overexpression of p53 (as previously shown) and reduction of COX activity in TIF-IA^{DATCreERT2} mutants (Fig. 20b).

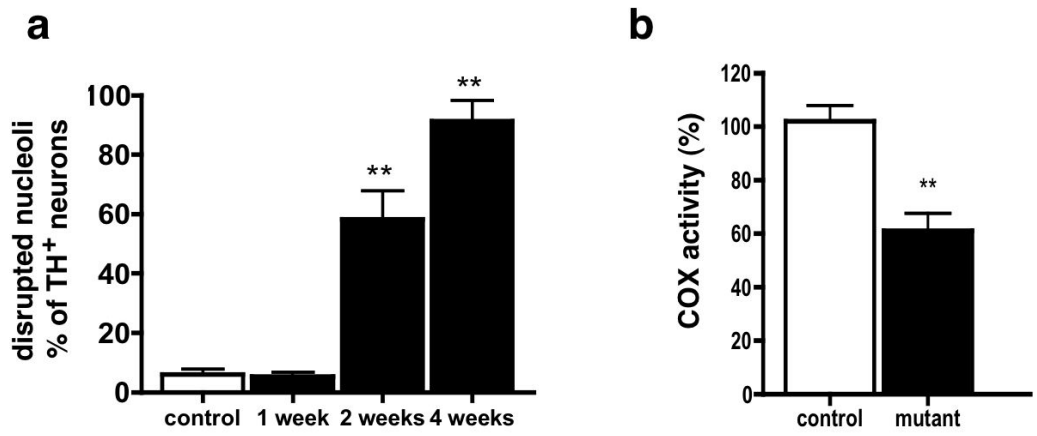

Figure 20: Disruption of the nucleolus is followed by increase in oxidative stress. (**a**) Quantification of nucleolar disruption in dopaminergic neurons in mice 1, 2 and 4 weeks after tamoxifen injection of control and TIF-IA^{DATCreERT2} mice, expressed as percent (%) of TH$^+$ neurons showing translocation of NPM (n=4). (**b**) 2 weeks after tamoxifen injection reduced COX activity in TIF-IA^{DATCreERT2} mutants is measured as optical density in comparison to control mice (n=3; **, $p<0.01$).

Impairment of mitochondrial activity causes higher levels of ROS (Finkel, 2005), which react with proteins, lipids and DNA. To analyze oxidative damage in TIF-IA^{DATCreERT2} mutants, the total number of TH^{+} neurons in controls and mutants that are positive for nitrosylated proteins (NITT)(St-Pierre, et al., 2006), neuroketals (NK) (Bernoud-Hubac, et al., 2001), and oxidized DNA (8-OHdG) (St-Pierre, et al., 2006) (Fig. 21a-f) was determined. Higher levels of nitrosylated proteins (Fig. 21a,b), neuroketals (Fig. 21c,d) and oxidized DNA (Fig. 21e,f) within dopaminergic neurons of TIF-IA^{DATCreERT2} mice were measured 4 weeks after tamoxifen injection (quantification shown in Fig. 21g). Remarkably, these alterations due to oxidative damage occur before structural changes in dopaminergic neurons or their projections to the striatum were observed (see Fig. 17a-o).

In order to test the hypothesis that nucleolar activity and mitochondrial signaling are tightly linked, TIF-IA^{DATCreERT2} and control mice were treated two weeks after Cre induction with MPTP or saline for 3 days, and dopaminergic neurons were analyzed one day after the last injection. A 15% reduction of TH^{+} neurons in control mice treated with MPTP was observed. As expected, TIF-IA^{DATCreERT2} mutants treated with saline showed no significant difference in the number of TH^{+} neurons compared to control mice. In contrast, TIF-IA^{DATCreERT2} mice treated with MPTP displayed a considerably higher loss of dopaminergic neurons (~42%) (Fig. 22) supporting the view that mitochondrial impairment affects the nucleolus.

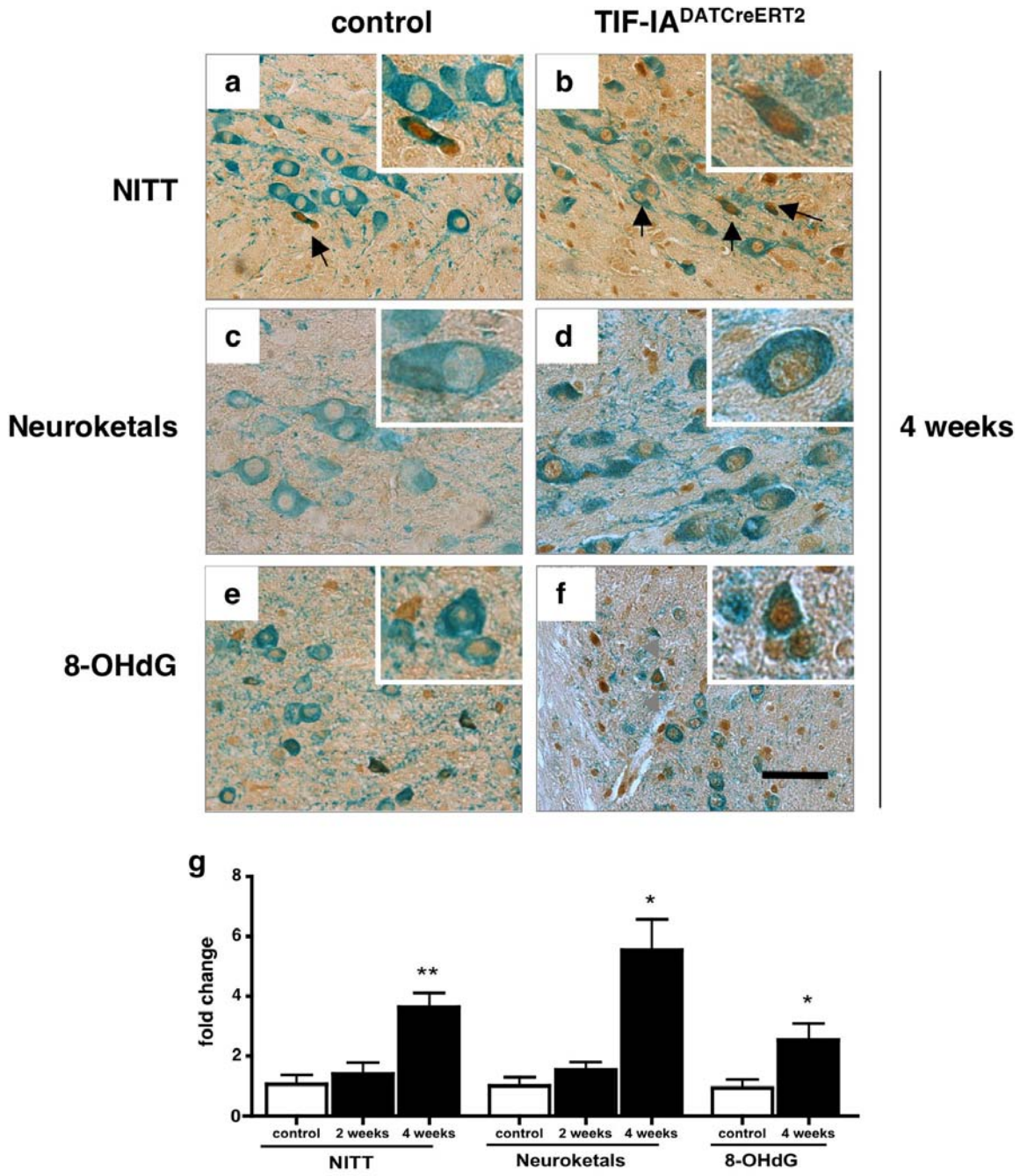

Figure 21: Nucleolar disruption leads to increased oxidative stress
(**c-h**) Brain sections through the ventral midbrain were analyzed for nitrosylated proteins (NITT) (**c,d**), neuroketals (**e,f**) and 8-hydroxydeoxyguanosine (8-OHdG) (**g,h**), as markers for ROS-induced cell damage (brown), in combination with TH staining (light blue) in order to identify dopaminergic neurons in mutants (**d,f,h**) compared to control littermates (**c,e,g**). Inserts show higher magnification of affected cells. (**i**) Quantification of dopaminergic neurons positive for oxidative stress markers in control and mutant mice 2 and 4 weeks after injection with tamoxifen. Differences are expressed as fold change in comparison to the mean of the controls at different stages. Higher levels of oxidative stress markers were observed in the mutants (n=4; *, $p<0.05$; **, $p<0.01$). Scale bar: c-h, 50μm.

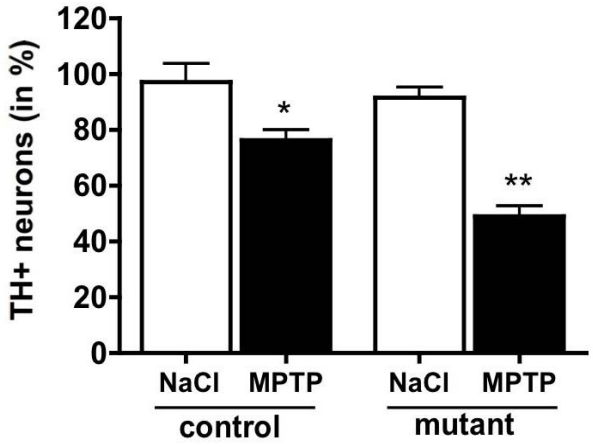

Figure 22: Linking nucleolar disruption with Parkinson's disease.
Effect of treatment with the neurotoxin MPTP on control and TIF-IA^{DATCreERT2} mutant mice is analyzed 2 weeks after tamoxifen injection by counting the number of TH^{+} neurons. Control mice receiving saline show moderate loss of dopaminergic neurons upon MPTP treatment, while TIF-IA^{DATCreERT2} mutants treated with the neurotoxin show a more severe reduction of TH^{+} neurons (n=5; *, $p<0.05$; **, $p<0.01$)

3.12 Increased nucleolar disruption in dopaminergic neurons of PD patients

The results obtained so far demonstrate that in dopaminergic neurons the nucleolus is involved in the oxidative stress response leading to mitochondrial impairment and the development of parkinsonism in TIF-IA^{DATCreERT2} mice. These observations prompted to examine the occurrence of nucleolar impairment in cases of human PD. Therefore four different patients suffering of PD (P1-P4) were analyzed and compared to midbrains from 'non-disease' humans (C1-C4) obtained from the German Brain Bank. Humans from different gender and at different stages of the disease according to Braak (see **Table 1**) were analyzed.

Table 1: Formalin-fixed, paraffin-embedded sections of the midbrain from 4 PD and 4 control cases were obtained from the German Brain Bank "Brain-Net". Demographic data:

	Age at death [y]	Post-mortem delay [h]	Disease duration [y]	Sex	Pathology stage according to Braak et al. 2003
P1	76	7.5	10	M	6
P2	63	24	16	M	4
P3	72	11	10	F	5
P4	71	20	>4	F	6
C1	54	9.5	NA	M	0
C2	60	6.5	NA	M	0
C3	86	24	NA	F	0
C4	66	10	NA	F	0

The perturbation of nucleoli in TH^+ neurons in clinically and pathologically confirmed cases of sporadic PD was quantified. In control sections the nucleolus is visible in a significantly higher percentage than in samples of PD (Fig. 23a,b). The quantification of our analysis reveals a strong increase in nucleolar disruption in PD cases (Fig. 23c). These findings show for the first time that the nucleolus is affected in PD, supporting the obtained results of the importance of the nucleolus in the neurodegenerative process occurring in PD.

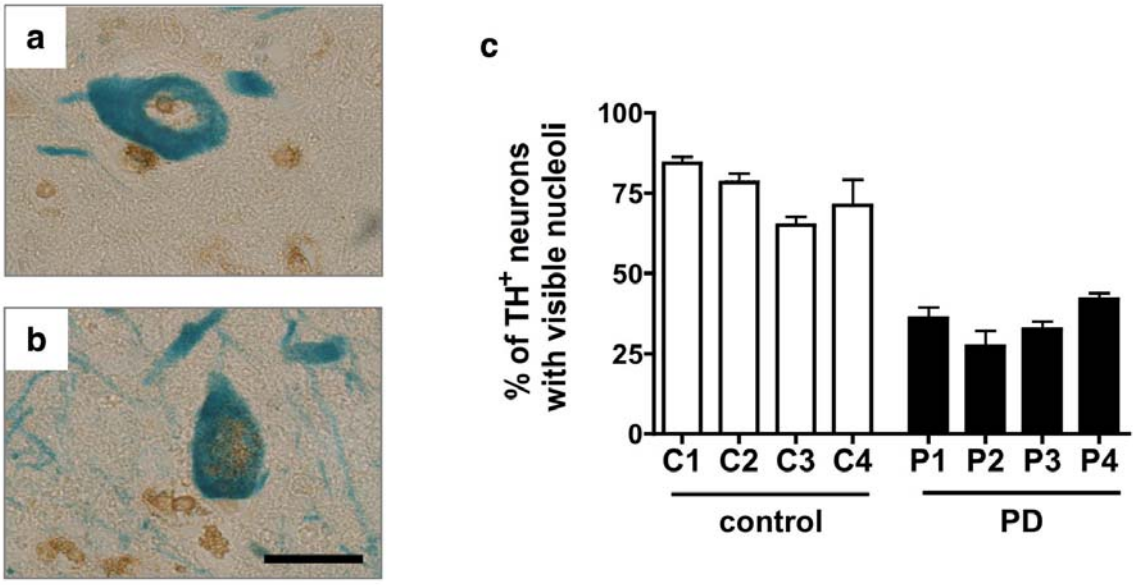

Figure 23: Nucleolar integrity is decreased in dopaminergic neurons of humans suffering from PD

(**a,b**) Example of human brain sections from controls (C1-C4) and PD patients (P1-P4) analyzed for nucleolar disruption (NPM, brown) in dopaminergic neurons (TH, blue). Dopaminergic neurons of controls display clearly visible nucleoli (**a**) while in PD patients they are often disrupted (**b**) (scale bar: b, c - 15μm). **(c)** Quantification performed on 4 PD cases (of different pathology progression) compared with controls. Samples from SN/VTA region of PD patients reveal a dramatic decrease of TH^+ neurons containing still visible nucleoli. Scale bar: c-h, 15μm.

4. Discussion

The nucleolus is a specialized sub-nuclear compartment where rRNA is synthesized, processed, modified and associated with ribosomal proteins and 5S rRNA before being exported to the cytoplasm. Apart from its traditional function as the ribosome-supplying organelle, the nucleolus has been shown to perform startling tasks in signal recognition and cell cycle regulation. One of the most intriguing novel roles of the nucleolus is the participation in sensing cellular stress signals and transmitting them to the p53 stabilization system (Boisvert, et al., 2007).

In MPTP-induced parkinsonism and presumably also in Parkinson's disease (PD), the main symptoms such as tremor and rigidity are attributed to the loss of dopaminergic neurons due to oxidative stress. In order to efficiently respond to hazardous conditions, cellular ROS sensors must exist to monitor oxidative stress and to respond towards it, for example, by regulating the expression of antioxidant genes or genes that promote cell death (Storz, 2006).

4.1 The nucleolus acts as a stress sensor in dopaminergic neurons

The capacity of the nucleolus to react upon different stress stimuli has been shown (Mayer and Grummt, 2005). In order to analyze if the nucleolus is able to sense and respond towards oxidative stress in dopaminergic neurons, the well established neurotoxin MPTP was used to induce cellular stress only in dopaminergic neurons of mice. MPTP itself is not toxic but capable of crossing the blood-brain barrier. Once inside the brain, MPTP is metabolized into the toxic cation 1-methyl-4-phenylpyridinium (MPP^+) by the enzyme monoamine oxidase B (MAO-B) of glial cells. The dopamine transporter shuttles MPP^+ into dopaminergic cells, where it interferes with complex I of the electron transport chain, a component of mitochondrial metabolism. This blockage of the respiratory process in the mitochondria causes the buildup of free radicals that contributes to cell death (Przedborski and Vila, 2003, Schober, 2004).

The finding that MPTP treatment not only impairs mitochondrial function in dopaminergic neurons, but also affects the structure and transcriptional activity of RNA polymerase I (Pol I), suggests a link between nucleolar and mitochondrial function in MPTP-induced parkinsonism. Moreover it provides additional evidence for the notion that ribosomal biosynthesis acts as a 'stress sensor' in dopaminergic neurons.

4.2 Generation of mice with artificial impairment of the nucleolus

The decrease in Pol I dependant transcription after MPTP-induced oxidative stress revealed a functional interrelationship between the nucleolus and mitochondria. The key factor responsible for conveying extracellular signals towards the Pol I apparatus is TIF-IA, a Pol I-associated factor that regulates the transcriptional output in response to diverse signaling events (Grummt 2003). It has been shown that in cells exposed to oxidative stress, TIF-IA is inactivated by JNK2-mediated phosphorylation and that rRNA synthesis is rapidly and efficiently shut-down (Mayer, et al., 2005, Yuan, et al., 2005).

Conditions that inhibit Pol I transcription perturb the structure of the nucleolus (Mayer and Grummt, 2005). Ribosomal proteins, including L5, L11 and L23, and proteins found in the nucleolus as $p19^{ARF}$ or nucleophosmin (Kurki, et al., 2004), (Lohrum, et al., 2003), are released from the nucleolus to the nucleoplasm, where they associate with MDM2. This association inhibits its activity and thereby stabilizes p53. It has been shown, that in mouse embryonic fibroblasts, depletion of TIF-IA leads to disruption of nucleoli, cell cycle arrest, upregulation of p53, and induction of apoptosis. RNAi-mediated knock-down of p53 can overcome proliferation arrest and apoptosis, reinforcing the central role of p53 in surveilling cellular health (Yuan et al., 2005).

To explore the consequence of perturbing this interrelationship nucleolar function was specifically ablated in dopaminergic neurons using Cre/loxP-mediated ablation of TIF-IA an essential factor for the recruitment of Pol I.

Dopaminergic neurons react upon TIF-IA ablation with nucleolar disruption, p53 upregulation and later on mutant mice display reduced weight gain, exhibit abnormal behavioral symptoms, includes slowness of movements, gait and posture disturbances and resting tremor resembling closely PD symptomatology.

Like in PD these locomotor abnormalities were associated with loss of dopaminergic neurons. While at birth mutant mice have a complete set of neurons, at later stages dopaminergic neurons were progressively lost. Intriguingly, dopaminergic neurons in the substantia nigra (SN) were more rapidly and strongly affected than those in the ventral tegmental area (VTA), mimicking the differential vulnerability of these two subpopulations of dopaminergic neurons in PD.

The dramatic loss of dopaminergic neurons in PD patients impairs dopamine production, leading to alterations of the neural circuits that regulate movement (Lang and Lozano, 1998b, Lang and Lozano, 1998a). Striatal dopaminergic innervations (characterized by TH immunoreactivity) were affected long before dopaminergic neurons were lost, representing another characteristic of PD. In addition the striatal dopamine content of TIF-IA^{DATCre} was reduced by 95% at 5 weeks of age. Reduced striatal dopamine transmission leads to impaired locomotor activity in TIF-IA^{DATCre} mutants, which we assessed using the accelerating rotarod assay.

Together, these results demonstrate that ablation of TIF-IA leads to progressive loss of dopaminergic neurons in the SN and VTA, reduction of the striatal dopamine content and severely impaired locomotor performance, closely mimicking the symptoms in PD.

4.3 Treatment with L-DOPA restores normal locomotor performance in transgenic mice

Parkinson's disease as a chronic disorder and the inevitable fact that at the present time there is no cure for it, medications or surgery provide the only form of treatment. The most widely used form of treatment is L-DOPA, the dopamine precursor (Birkmayer and Hornykiewicz, 1961). In order to verify if treatment with L-DOPA can rescue TIF-IA^{DATCre} mice from death, L-DOPA was injected either i.p. or continuously released by implanted pellets.

While mutants without treatment with L-DOPA did not gain weight and died early, mutant mice treated with L-DOPA gained weight and were rescued from death. Moreover, increased growth of TIF-IA^{DATCre} mice was achieved 6 weeks after continuous treatment by implanting subcutaneous pellets releasing a constant amount of L-DOPA. The data obtained demonstrate the responsiveness of TIF-IA^{DATCre} mice towards L-DOPA administration, recapitulating another important feature of PD.

4.4 Impairment of nucleolar function affects mitochondrial activity and induces oxidative stress.

Given the crucial role of mitochondrial dysfunction in PD and the interesting similarity of our model towards PD symptomatoloy, it became increasingly interesting to see whether nucleolar perturbation upon TIF-IA ablation results in mitochondrial dysfunction and whether oxidative stress is involved in damage of dopaminergic neurons in TIF-IA^{DATCre} mice (Dauer and Przedborski, 2003).

To elucidate the molecular mechanism that triggers loss of dopaminergic neurons after TIF-IA depletion, we first assessed whether ablation of TIF-IA in dopaminergic neurons leads to alterations of nucleolar structure. TIF-IA^{DATCre} embryos at E18.5 were used and nucleolar integrity by immunofluorescence using antibodies against nucleophosmin and tyrosine hydroxylase monitored. In control cells, NPM is localized within the nucleoli, whereas in TIF-IA^{DATCre} mutants NPM is distributed throughout the nucleoplasm and p53 is

overexpressed. Mitochondrial impairment can be detected (among others) by reduced activity of the cytochrome c oxidase (COX) (Bender, et al., 2006, Ekstrand, et al., 2007). And indeed, at E18.5 TIF-IA^{DATCre} mutants showed strongly reduced levels of COX activity in the ventral mesencephalic area compared to control mice, indicating that loss of TIF-IA function affects mitochondrial activity.

A constitutive Cre recombinase mouse line was used, which shows onset of expression before the development of the brain is completed (Parlato, et al., 2006). Therefore phenotypical changes can arise from interferences of the mutation during brain development and/or from the deficiency of the respective protein in dopaminergic neurons. Although no difference of the total dopaminergic neuronal population at birth was visible, some alterations happen during embryogenesis, like nucleolar disruption and p53 upregulation due to ablation of TIF-IA.

4.5 Generation of mice expressing an inducible Cre recombinase specifically in dopaminergic neurons

In order to assess in more detail the sequence of events that link nucleolar with mitochondrial function in the adult mice and to avoid developmental deficits or compensatory effects, mutant mice expressing an inducible Cre recombinase have been generated, allowing the spatio-temporal control of the Cre-mediated recombination. The expression of the transgene, resembling the expression of the endogenous gene independently of the integration site, was ensured by the use of a BAC vector (bacterial artificial chromosome), containing large regions of genomic DNA with almost all regulatory elements of the gene (Casanova, et al., 2001, Parlato, et al., 2006). To target dopaminergic neurons exclusively, the regulatory elements of the mouse dopamine transporter gene were used to express the CreER^{T2} fusion protein in dopaminergic neurons of the adult mouse brain.

Nuclear translocation of the CreER^{T2} is achieved by applying tamoxifen, which then allows Cre-mediated recombination (Indra, et al., 1999, Erdmann, et al., 2007). Using the ROSA26 Cre reporter the effective temporal regulation of

CreER^{T2} activity by tamoxifen treatment was demonstrated. In the absence of the ligand very low recombination was detectable by whole mount staining only within the SN/VTA region. Treatment with tamoxifen resulted in strong recombination within dopaminergic neurons of the SN and the VTA. In addition, one of the analyzed lines displayed recombination in the olfactory bulb and the arcuate nucleus reflecting most precisely reported locations of dopaminergic neurons, which was then used to generate TIF-IA mutants.

4.6 Inducible ablation of TIF-IA leads to nucleolar disruption

The DATCreER^{T2} transgene was successfully employed in TIF-IA^{DATCreERT2} mice to achieve ablation of TIF-IA in dopaminergic neurons. Cre-induced inactivation of TIF-IA in adult mice (2 months old) leads to a similar neurodegenerative process as seen in PD (Conforti, et al., 2007). 13 weeks after induction of Cre recombinase by tamoxifen, loss of TH immunoreactivity in the striatum was associated with a major loss of dopaminergic neurons, culminating in an almost complete loss of dopaminergic neurons 21 weeks after induction. Interestingly, reduced TH immunoreactivity in the striatum precedes loss of the corresponding dopaminergic cells in the SN. This phenomenon has also been observed in parkinsonism (Lang and Lozano, 1998a, Lang and Lozano, 1998b). Monitoring of TIF-IA^{DATCreERT2} mutants revealed a progressive decline of locomotor activity, reflecting the decreased number of dopaminergic neurons after Cre-mediated TIF-IA ablation.

Summarizing, conditional and inducible disruption of nucleolar integrity in dopaminergic neurons by specific ablation of the transcription initiation factor TIF-IA results in many of the hallmarks of parkinsonism, including progressive, but differential loss of dopaminergic neurons in the SN and VTA, progressive depletion of striatal dopamine projections, pronounced reduction of striatal dopamine content, responsiveness to L-DOPA treatment as well as marked deficiencies in animal motor performance (tremor, rigor, bradykinesia).

4.7 Increased expression of Lewy body components

Another pathological characteristic of PD, besides loss of nigrostriatal dopaminergic neurons, is the presence of intraneuronal proteinaceous cytoplasmic inclusions, termed Lewy bodies. This abnormal deposition of protein in brain tissue is a feature of several age-related neurodegenerative diseases and not exclusive for PD. The composition and location of protein aggregates differ from disease to disease. It has been shown that the Lewy bodies in PD are a composition of parkin, synphillin, ubiquitin and alpha-synuclein (Saudou, et al., 1998, Cummings, et al., 1999, Dauer and Przedborski, 2003). Analysis on TIF-IA^{DATCreERT2} mice revealed a considerable difference in expression of parkin, synphilin and α-synuclein. This indicates a shift of protein expression in mutant mice during the neurodegenerative process. Since currently existing genetic animal models for this neurodegenerative disease have not been able to reproduce all the features of PD, the mouse mutants generated here provide a new tool to explore new treatments or implantation techniques for PD.

4.8 Linking nucleolar activity and mitochondrial integrity

Besides generating a valuable tool for PD research, another important and unexpected finding of this study was that the disintegration of the nucleolus by ablation of TIF-IA leads to mitochondrial impairment associated with increased oxidative stress before the survival of SN/VTA neurons is affected. The inducible mouse model (TIF-IA^{DATCreERT2}) enables to dissect different events happening after TIF-IA loss. So, one week after Cre-mediated ablation of TIF-IA a dramatic increase in the number of disrupted nucleoli in TH^{+} neurons of mutant mice was visible and associated with p53 upregulation.

Interestingly, p53 has been shown to accumulate in the SN of sporadic cases of PD (Nair, et al., 2006) and in other neurodegenerative diseases, such as Huntington`s (striatum) or Alzheimer`s diseases (cortex) (Bae, et al., 2005, Alves da Costa, et al., 2006). Furthermore, the importance of p53-dependent cell death in dopaminergic neurons are strengthened by studies showing that p53$^{-/-}$ mice are resistant to MPTP toxicity (Trimmer, et al., 1996).

Two weeks after activation of the Cre recombinase, mitochondrial impairment was detectable by measuring COX activity in TIF-IA^{DATCreERT2} mutants. The impairment of mitochondrial activity causes increasing ROS levels, which in turn react during the detoxification process with proteins, lipids or DNA. Higher levels of ROS scavenging products like nitrosylated proteins, neuroketals and oxidized DNA, within dopaminergic neurons of TIF-IA^{DATCreERT2} mice were measured 4 weeks after tamoxifen injection. Remarkably, the development of the abnormalities in mitochondrial function following blockade of rRNA signaling occur long before the loss of dopaminergic neurons begins (Fig. 24).

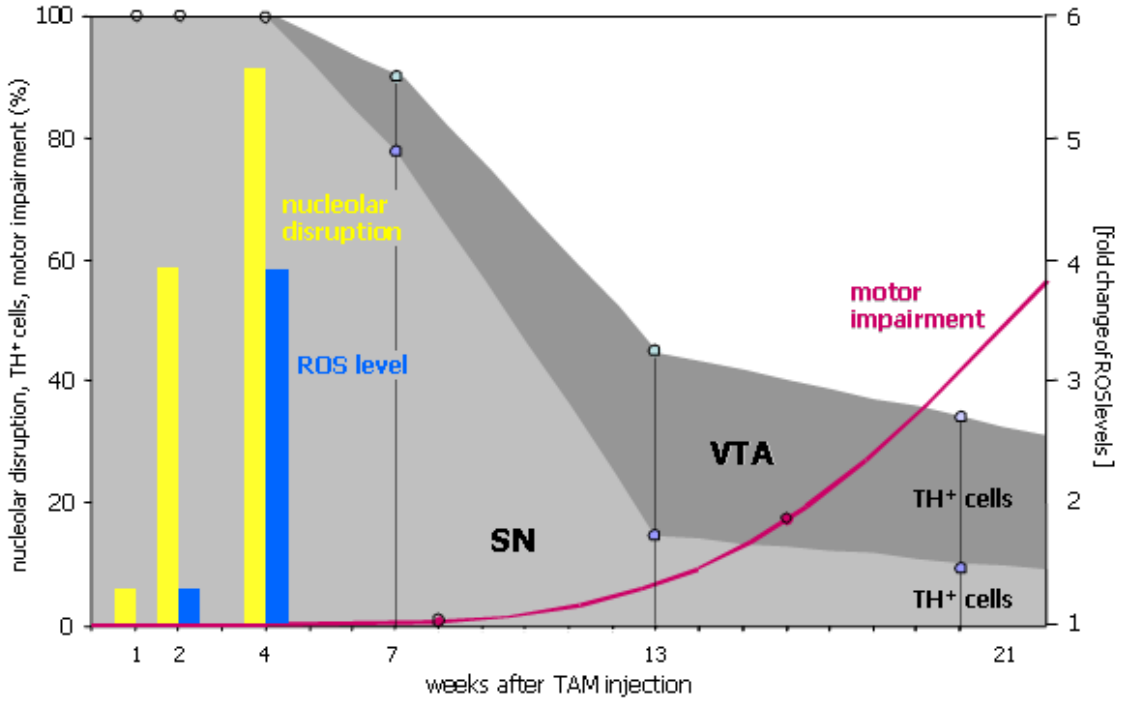

Figure 24: Sequence of events observed in TIF-IA^{DATCreERT2} mutants. Disruption of nucleolar integrity, clearly observed already 2 weeks after induction of the mutation by tamoxifen injection is followed by increased levels of ROS. This leads to neurodegeneration of dopaminergic neurons within SN and – after some delay – within VTA. When the amount of the cells in SN is reduced to approx. 20%, the animals start to show increased motor impairment (revealed by rotarod test).

In the context of control of the oxidative stress response, it is worth mentioning that the adaptor protein $p66^{Shc}$, which directly stimulates ROS production (Orsini, et al., 2004, Giorgio, et al., 2005), has been shown to act as a downstream target of p53 and to be crucial for p53-dependent mitochondrial ROS production. Interestingly, $p66^{Shc}$ null mice are resistant to paraquat, a pesticide that induces selective dopaminergic degeneration (Dauer and Przedborski, 2003). It remains to be elucidated how nucleolar disruption and p53 upregulation directly affects mitochondrial activity.

In order to test the hypothesis that nucleolar activity and mitochondrial signaling are tightly linked, TIF-$IA^{DATCreERT2}$ and control mice were treated two weeks after Cre induction with MPTP or saline. TIF-$IA^{DATCreERT2}$ mice treated with MPTP displayed a considerably higher loss of dopaminergic neurons than control mice treated with MPTP, supporting the view that mitochondrial impairment affects the nucleolus. It seems that within dopaminergic neurons higher ROS levels are sensed by the nucleolus, as indicated by the pronounced decrease of RNA polymerase I activity one day after MPTP treatment. In turn inhibition of transcription disturbed nucleolar structure, causing release of nucleolar components, triggering p53 stabilization, leading to the impairment of mitochondrial activity and finally promoting cell death. Although other mechanisms linking nucleolar and mitochondrial function cannot be excluded, the data suggest the existence of a self-reinforcing loop that can be activated at several levels once a threshold of injurious stimuli is passed (Fig. 25).

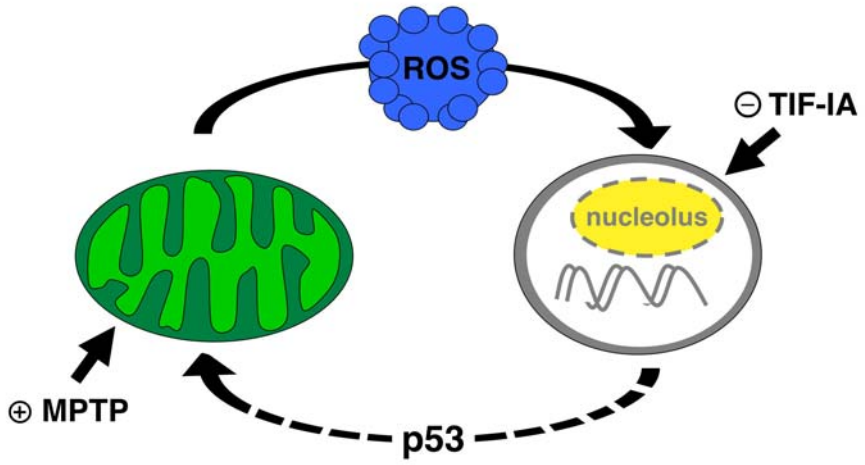

Figure 25: Schematic representation of a model linking mitochondria and nucleolar activity.
Toxic insults directed to mitochondria, such as the treatment with MPTP, increase the production of ROS. The nucleolus responds by downregulating rRNA synthesis. By TIF-IA ablation, changes in nucleolar integrity and activity alter the turnover of p53, leading to impairment of mitochondria and increased oxidative stress. Increased p53 levels may activate the apoptotic machinery at the mitochondria, leading to even higher accumulation of ROS and causing a sustained stress eventually lethal for the cell.

This model is further supported by the observation that an intact nucleolus is crucial for the resistance to oxidative insult produced by MPTP treatment. The mitochondrial damage following TIF-IA loss leads to increased ROS production, which will further worsen the mitochondrial damage. Once this vicious cycle is adopted, increasing levels of free radicals progressively consume the antioxidant capacity, ROS production overcomes its removal and further mitochondrial deficiencies will ensue.

4.9 Increased nucleolar disruption in dopaminergic neurons of PD patients

The phenotype of the mutants lacking TIF-IA suggests a novel and unpredicted role of the nucleolus and its function in the pathophysiological processes involved in parkinsonism. This notion is substantiated by the observation that PD patients display increased perturbation of nucleoli in dopaminergic neurons compared to control cases.

Based on the findings reported here, a correlation between impaired nucleolar-dependent activities and increased sensitivity to oxidative stress as observed in some genetic forms of PD is likely to exist. It has been reported that the protein DJ-1, associated with familial cases of PD, inhibits the tumor suppressor PTEN (Kim, et al., 2005b). PTEN in turn is known to inhibit the activity of RNA polymerase I (Zhang, et al., 2005). Therefore, a very attractive possibility is that loss of DJ-1 in PD patient results in increased PTEN activity and inhibition of rRNA synthesis. Disruption of nucleolar integrity in PD patients would make neurons more vulnerable to oxidative stress. In this context it is interesting that DJ-1-deficient mice are also hypersensitive to MPTP (Kim, et al., 2005a) and that inactivation of DJ-1 in Drosophila melanogaster increases sensitivity to oxidative stress (Yang, et al., 2005).

Given the crucial role of the nucleolus in the oxidative stress response, it is reasonable to propose that TIF-IA ablation and subsequent nucleolar impairment in the dopaminergic neurons of mutant mice mimic, at least partially, the chain of events leading to cell death in PD. Therefore, it is important to unravel in which way structural and functional perturbations of the nucleolus are involved in the development of the pathophysiology of PD. Thus, these studies are of clinical importance to develop procedures aimed to alleviate the consequences of this neurodegenerative disease.

5. Materials and Methods

5.1 Materials

5.1.1 Chemicals and enzymes

Chemicals and enzymes were in general purchased from the following companies:

Chemicals:

BioRad, Munich
Difco, Detroit
Fluka, Neu-Ulm
VWR International, Darmstadt
Roth, Karlsruhe
Serva, Heidelberg
Sigma-Aldrich, Munich
Applichem, Darmstadt

Enzymes:

Roche, Mannheim
New England Biolabs, Schwalbach
Invitrogen, Karlsruhe
Stratagene, Heidelberg
Promega, Heidelberg

5.1.2 Standard solutions

10x PBS (phosphate buffered saline)
1,37 M NaCl
100mM Na_2HPO_4
27mM KCL
20mM KH_2PO_4
pH 7.2
optional → 1ml DEPC/1l, stirred and autoclaved

TE
10mM Tris/HCl, pH 8
1mM EDTA, pH 8

50x TAE (Tris acetate EDTA buffer)
2M Tris base
50mM EDTA
250mM NaAc
pH 7.8 (glacial acidic acid)

20x SSC (standard sodium citrate buffer)
3M NaCl
0,3M sodium citrate
pH 7

10x TBE
2M Tris
250mM NaAc
50mM EDTA
pH 7.8 (glacial acetic acid)

5.1.3 Plasmids

PIndu: The plasmid generated and provided by Dr. Erich Greiner (Evotec, Germany) was used to clone the construct for the knock-in of a Cre^{ERT2} cassette at the ATG of the dopamine transporter gene present on a large genomic fragment (BAC vector) by homologous recombination in bacteria. The plasmid contains a cassette encoding a fusion protein consisting of the codon-improved Cre recombinase (Shimshek, et al 2002) and a mutated ligand-binding domain of the human estrogen receptor (Feil et al, 1997). In addition the plasmid harbors an ampicillin resistance cassette flanked by two FRT sequences, which can therefore be removed by the Flp recombinase.

5.2 Plasmid constructs and probes

DNA fragments were generally cloned into pBluescript II KS (+/-) vector (Stratagene)

5.3 Standard techniques in molecular biology

5.3.1 Cloning into plasmid vectors and sequencing

Cloning of DNA fragments into plasmid vectors was performed following the established standard protocols in Sambrok et al. (1989) and is therefore not described here. Methods to obtain DNA fragments or vectors and to clone different plasmid constructs included digestion with restriction enzymes, dephosphorylation of DNA ends with Shrimp alkaline phosphatase (Roche), phosphorylation of DNA ends with polynucleotidekinase, as well as, ligation of DNA fragments using T4-DNA-polymerase. Isolation of DNA fragments out of agarose gels was performed using the Qiaquick Gel-Extraction Kit (Qiagen) according to manufacturer's instruction. Competent bacteria of the strain E.Coli NM554 were generally transformed by heat-shock at 42°C. Recombinant plasmid DNA was then isolated from the bacteria as described before.

5.3.2 Isolation of DNA

5.3.2.1 Miniprep of plasmid from bacteria DNA from bacteria

This method was adapted from Holmes and Quigley, 1981 and is suitable for preparation of small amounts of DNA to screen a large number of bacterial clones. 1ml of an O/N bacterial culture was centrifuged for 30s at 13.000rpm and resuspended in 400µl STET buffer. After incubation of the preparation with 32µl lysozyme solution (10µl/ml), the Miniprep was heated up to 95°C for 2min, cooled down at 4°C for 30min and subsequently centrifuged for 15min, at 4°C with 14.000rpm. The pellet was removed using a blue tip and 800µl $EtOH_{abs}$ were added to the remaining supernatant followed by 10min incubation at RT. The preparation was centrifuged afterwards for 10min at 4°C with 14.000rpm, the supernatant was removed and the pellet was washed once with 70% EtOH, subsequently air dried and dissolved in 100µl TE.

STET buffer	
50mM	Tris/Hcl, pH8
50mM	EDTA
5%	Trition-X-100
8%	sucrose

5.3.2.2 Miniprep of BAC DNA

The size of a BAC (about 150kb circular supercoiled DNA) and its low abundance in a bacterial culture (1-2 copies/bacterium) requires a different preparation method than the one used for plasmid DNA. The bacterial colonies were inoculated in 2ml LB medium containing chloramphenicol (25µl/ml). After centrifugation (4000rpm, 10min, 4°C), the culture was resuspended in P1, the bacterial membrane was destroyed by alkaline lysis with P2 and the lysate was neutralized using P3 (P1, P2, P3 buffers, Qiagen). The preparation was then centrifuged (14.000rpm, 10min, 4°C), the supernatant was transferred into a new tube and 600µl isopropanol were added. After centrifugation (14.000rpm, 10min, 4°C) the pellet was washed in 70% EtOH, dried and resuspended in 40µl TE. The concentration and quality

was verified by gel electrophoresis after appropriate restriction-digestion of the BAC.

5.2.2.3 Midiprep of BAC DNA

Midiprep of BAC DNA was performed using Q20-columns and regents from Qiagen. The BAC-positive bacterial colonies were inoculated in 50ml LB-medium containing chloramphenicol (25µl/ml). The preparation of the neutralized lysate was performed as described for Miniprep with 5ml of each of the buffers. The lysate was centrifuged at 4000rpm at 4°C for 20min and filtered through cheesecloth. The DNA was precipitated by addition of 10ml isopropanol and subsequent centrifugation (4000rpm, 4°C, 20min). The pellet was resuspended in 1ml QBT buffer (Qiagen) and applied to a Q20-column (equilibrated with 1ml QBT) for 5min. After 3 washing steps with 2ml QC buffer (Qiagen), the DNA was eluted twice with 800µl of preheated (70°C) QF buffer (Qiagen) and precipitated with 560µl isopropanol followed by 15min centrifugation with 14.000 at 4°C. The pellet was washed with 70% EtOH, dried and resuspended in 25µl TE. The concentration and quality was verified by gel electrophoresis after appropriate restriction digestion of the BAC: For preparation of the BAC DNA for microinjection the pellet was resuspended in 10µl TE, incubated for 10min at RT and exonuclease activity was then inactivated by 15min incubation at 65°C.

5.4 Generation of transgenic mice

5.4.1 Modification of a BAC by homologous recombination in bacteria

Recombinant DNA molecules can be generated by homologous recombination in bacteria (ET-cloning) using the method of Copeland and Court (Lee, et al., 2001). This method allows the integration of a linear DNA sequence into a homologous region of an acceptor vector.

The BAC used to generate for the DATCre transgene (Parlato, et al., 2006) was modified by homologous recombination in EL250 cells to insert a cassette encoding a fusion protein ($CreER^{T2}$) consisting of a codon-improved Cre

recombinase (Cre) (Shimshek, et al., 2002) and a mutated ligand-binding domain of the human estrogen receptor (ER^{T2}) (Feil, et al., 1997) as well as an ampicillin resistance cassette flanked by two FRT sites.

5.4.2 Preparation of competent bacteria for transformation with the BAC

Single colonies of EL250 bacteria (Copeland/Court) were inoculated in 5ml LB-medium at 32°C. 2ml of the O/N culture were transferred into 50ml LB-medium and incubated at 32°C for 3-4hrs. When cells reached the log phase (OD=0.4-0.5), they were cooled on ice and centrifuged for 10min at 4°C, 4000rpm. The cell pellet was resuspended in 50ml of ice-cold 10% glycerol and centrifugation as well as resuspension in 10% glycerol was repeated twice. After the last washing, the supernatant was poured off. The pellet was resuspended in the remaining 10% glycerol resulting in a final volume of 0.6-0.7ml. 50µl aliquots of the cells were transferred into pre-cooled Eppendorf tubes and frozen in liquid nitrogen.

5.4.3 Re-transformation of the BAC

Miniprep of the BAC was prepared as described above. The competent EL250 cells were thawed on ice and the electroporation cuvettes were pre-cooled on ice. A series of 1µl, 2µl and 5µl of the BAC miniprep were added to 50µl competent cells respectively, followed by electroporation at 2.3kV (BioRad Gene Pulser, 25µF with Pulse controller set to 200Ω). 1ml LB-medium was added afterwards, the cells were transferred into eppendorf tubes and incubated for 1h at 32°C. Finally 100µl of the cells were plated directly on LB-plates containing chloramphenicol (25µg/ml), whereas the remaining cells were centrifuged, resuspended in 100µl LB-medium and plated on a second chloramphenicol plate.

5.4.4 Preparation of competent bacteria for homologous recombination

Single colonies were picked from EL250 bacteria containing the desired BAC clone and inoculated in 5ml LB-medium/chloramphenicol (25µg/ml) at 32°C O/N. Next day 2ml of the O/N culture were transferred into 50ml LB-medium and incubated at 32°C for 3-4hrs. When cells reached the log phase (OD=0.4-0.5), the RED-recombination system was induced by 15min shaking in a 42°C water bath. After incubation, the cells were rapidly cooled down and incubated on ice for 10-40min. Subsequent washing steps with 10% glycerol, resuspension and freezing in 50µl aliquots followed, as described previously.

5.4.5 ET recombination and removal of the ampicillin resistance cassette

0.1pmol of the linearized and purified CreER^{T2} construct were electroporated into the RED-induced bacteria at 2.3kV (BioRad Gene Pulser, 25µF with Pulse controller set to 200Ω). The cells were incubated in additional 1ml LB-medium for 1h as described before (5.3.1.3.) and plated on LB-plates containing chloramphenicol (25µg/ml) and ampicillin (50µg/ml) followed by incubation at 32°C (at least for 16hrs). Colonies were picked and BAC minipreps were performed as described, followed by diagnostic digestion with frequent cutting enzymes to verify successful ET-recombination.

The CreER^{T2} construct contains an ampicillin resistance cassette to select for the BAC that underwent homologous recombination with the construct. After homologous recombination in bacteria the resistance cassette was removed from the modified BAC. Since the cassette is flanked by two FRT sequences, it can be excised by Flp-recombinase, which can be induced in EL250 bacteria by L-arabinose (Sigma). Of the recombined clone 5ml O/N culture (containing 25µg/ml chloramphenicol) were incubated at 32°C and the next day a 1:50 dilution of the culture was prepared and incubated at 32°C until cells reached OD of 0.5. Then cells were treated for 1h with 0.1% L-arabinose at 32°C, diluted 1:10, incubated an additional hour and were plated onto chloramphenicol (25µl/ml) LB-plates followed by incubation at 32°C. After O/N

incubation, colonies were picked and transferred into 5ml LB medium (containing 25µg/ml chloramphenicol). After O/N incubation, a small aliquot of the culture was incubated for few hours in LB-medium containing chloramphenicol (25µl/ml) and ampicillin (50µg/ml) to verify the loss of the ampicillin resistance cassette by negative selection. From a culture that was not growing in ampicillin LB-medium, a BAC Miniprep was performed with subsequent diagnostic digestion by analytical pulse-field gel electrophoresis.

5.4.6 Preparative and analytical pulse-field gel electrophoresis

The modified genomic fragment containing the $CreER^{T2}$ knock-in at the ATG of the DAT gene was released from the BAC backbone by NotI digestion. For this purpose, 100µg BAC DNA, isolated according to the BAC Midiprep protocol, were digested O/N with NotI and heat inactivated the next day for 10min at 65°C. The linearized recombined genomic insert was purified by preparative pulse-field gel electrophoresis (PFGE) (Schedl, et al., 1993). 50µg of the digested BAC DNA were resolved on a 1% Sea-plug low-melting-point agarose (Sigma) gel in 0.5xTAE running buffer using the following parameters: initial t_{switch} = 0.2s, final t_{switch} = 12s, included angle a = 106°, $|E|$ = 6V/cm, I ≅ 140mA, total time t= 14h. For determination of the gel area to be cut out, only the gel parts containing the marker were stained with ethidiumbromide. The gel piece containing the genomic insert of the BAC was isolated according to the marker-bands and the agarose was digested with µ-agarose (Sigma) at 40°C for 20min. Non-digested agarose was removed and the DNA was purified using centrifugation cartridges. For microinjection of the modified genomic fragment into mouse oocytes, the DNA was further purified by dialysis with microinjection buffer for 2-3hrs. The concentration of the DNA preparation was estimated on a 0.8% agarose gel using various amounts of a linearized plasmid of the same size. The integrity of the DNA sample was verified by analytical PFGE, which was performed like the preparative PFGE with the exception that the entire gel, prepared with standard agarose, was stained with ethidiumbromide in order to detect the DNA fragments.

Agarase buffer

10mM	Tris/HCl, pH 6.5
1mM	EDTA
100mM	NaCl
30µM	spermine (Sigma)
70µM	spermidine (Sigma)

Microinjection buffer

10mM	Tris/HCl, pH 7.5
0.1M	EDTA
100mM	NaCl

5.4.7 DNA microinjection in mouse oocytes

The microinjection of DNA into mouse oocytes was performed according to the protocol of Hogan (Hogan et al., 1994). Superovulated fertilized FVB/N females were used as source of oocytes. To induce superovulation, females were first injected intraperitoneally with PMS-gonadotropin (Sigma) and 48 hours later with chorion-gonadotropin (Sigma). After administration of chorion-gonadotropin, the females were mated with FVB/N males and were analyzed for the presence of a vaginal plaque the following morning. Positive females were sacrificed the morning after the mating by cervical dislocation, the oviducts were removed and transferred into 37°C-warm M2-medium. Oocytes were isolated and cumulus cells surrounding the oocytes were removed by hyaluronidase treatment (100mg/ml in M2-medium; Sigma). Oocytes were then rinsed in M2-medium, transferred into M16-medium and incubated at 37°C. For microinjection, 30 oocytes were transferred in an injection syringe containing M2-medium and placed under a microscope with two micromanipulator setups connected to a hydraulic control system (Eppendorf femtoJet). Oocytes were fixed with a blunt pipette and the tip of the injection needle was filled with the prepared DNA. The DNA was injected at a concentration of 1µg/µl or 2µg/µl in a volume of 1-2pl into the larger male pronucleus and oocytes were subsequently incubated for 2hrs in M16-medium at 37°C and controlled for their vitality.

To transfer the oocytes into foster mothers, pseudo pregnant FVB/N females (mated with vasectomized males one day before) were intraperitoneally injected with Ketavet and Rompun (0.01ml of a 1:10 in PBS diluted solution per g bodyweight) to anesthetize the animals. To transfer the oocytes, the operation site was desinfected with EtOH, the abdominal cavity was opened and the oviduct was pulled out. Using a binocular the oocytes were injected into the oviduct, it was returned to the abdominal cavity and the wound was closed with clamps. The females delivered 18 days after the surgery and 5-15% of the offspring were expected to be transgenic.

M2-medium

20ml	10xA
3.2ml	10xB
2ml	33mM sodium pyruvate (Serva)
2ml	171.4mM $CaCl_2$ $(H_2O)_2$
16.8ml	250mM HEPES (sodium salt, Sigma)
156ml	H_2O
800mg	BSA (Serva)
pH 7.4	(NaOH)

M16-medium

20ml	10xA
20ml	10xB
2ml	33mM sodium pyruvate (Serva)
2ml	171.4mM $CaCl_2$ $(H_2O)_2$
156ml	H_2O
800mg	BSA (Serva)
pH 7.4	NaOH)

10xA

47mM	NaCl
47.75mM	KCl
11.9mM	KH_2PO_4
232.8mM	sodium lactate (Sigma)
55.6mM	D-glucose
0.6g/l	penicillin (Seromed)
0.5g/l	streptomycin (Seromed)

10xB

250mM	$NaHCO_3$
max. 5mg	phenolred

5.5 Genotyping

All primers used for PCR were ordered at MWG Biotech AG, Munich.

5.5.1 Isolation of genomic mouse DNA by NID lysis buffer

The DNA used for the PCR was obtained as followed: from adult mice we used a piece of the tail (about half centimeter), from embryos the whole tail and from organs a small piece (approximately 100 mm^3). The pieces were additionally washed in PBS in order to limit possible contaminations between tissues of different samples. Afterwards they were digested over-night at 56°C in 200µl of NID buffer, which is a non-ionic detergent buffer, added with 2µl of proteinase K (10mg/ml). The proteinase K was inactivated the following day at 95°C for 15 min. After collecting the possible condense by centrifugation, the NID-lysates were used for genotyping by PCR.

NID buffer

50 mM	KCl
10 mM	Tris pH8.3
2 mM	$MgCl_2$
0.1 mg/ml	gelatine
0.45%	NP40
0.45%	Tween 20
1 mg/ml	proteinase K

5.5.2 Polymerase Chain Reaction (PCR)

The PCR was done in a Thermocycler Gene Amp PCR system 9700 (Applied Biosystems) with the following primers and protocols:

DATCre transgene

5`-primer/Cre212: 5`-CTGCCAGGGACATGGCCAGG-3'
3`-primer/Cre213: 5`-GCACAGTCGAGGCTGATCAGC-3'
Expected PCR products: wild-type: no band
mutant: 500bp

NIDprep-DNA	**2 µl**
10x buffer with $MgCl_2$	**2,5 µl**
dNTPs (5mM)	**2 µl**
Primer 212 (10pmol/µl)	**1 µl**
Primer 213 (10pmol/µl)	**1 µl**
Taq-polymerase (1U/µl)	**1 µl**
sterile water	**16,5 µl**
Final volume	**25 µl**

PCR condition			
	95°C	5 min	
	95°C	1 min	35 x
	60°C	1 min	
	72°C	2 min	
	72°C	10 min	

DATCreER^{T2} transgene:

Cre2 Fw: 5`-GGC TGG TGT GTC GTC CAT CCC TGA A-3'
Cre2 Rev: 5`-GGT CAA ATC CAC AAA GCC TGG CA–3'
Expected PCR products: wild-type: no band
mutant: 405bp

NIDprep-DNA	**2 µl**
10x buffer with $MgCl_2$	**2,5 µl**
dNTPs (5mM)	**2 µl**
Cre2 Fw (10pmol/µl)	**1 µl**
Cre2 Rev (10pmol/µl)	**1 µl**
Taq-polymerase (1U/µl)	**1 µl**
sterile water	**16,5 µl**
Final volume	**25 µl**

PCR condition			
	95°C	3 min	
	95°C	45 sec	35 x
	60°C	1 min	
	72°C	2 min	
	72°C	10 min	

ROSA-LacZ transgene:

ROSA-1: 5`-TCT GCT GCC TCC TGG CTT CTG A-3'
ROSA-2: 5`-CCA GAT GAC TAC CTA TCC TCC CA –3'
ROSA-3: 5`-AAG CGC ATG CTC CAG ACT GCC T –3'
Expected PCR products: wild-type: 270bp
mutant: 420bp

NIDprep-DNA	**2 µl**
10x buffer with $MgCl_2$	**2,5 µl**
dNTPs (5mM)	**2 µl**
ROSA-1 (10pmol/µl)	**1 µl**
ROSA-2 (10pmol/µl)	**1 µl**
ROSA-3 (10pmol/ml)	**1 µl**
Taq-polymerase (1U/µl)	**1 µl**
sterile water	**16,5 µl**
Final volume	**25 µl**

PCR condition			
	95°C	3 min	
	95°C	45 sec	35 x
	63°C	1 min	
	72°C	2 min	
	72°C	10 min	

TIF-IA –locus:

TIF-IA FWD: 5`-CCG GTG GTC CTG CTT ACA CTA GAGATGTGG-3'
TIF-IA REV: 5`-AATATAATT TGC AGC AGCCTGCCTGATGATGG–3'
Expected PCR products: wild-type: 680bp
mutant: 760bp

NIDprep-DNA	**2 µl**
10x buffer with $MgCl_2$	**2,5 µl**
dNTPs (5mM)	**2 µl**
TIF-IA FWD (10pmol/µl)	**1 µl**
TIF-IA REV (10pmol/µl)	**1 µl**
Taq-polymerase (1U/µl)	**1 µl**
sterile water	**16,5 µl**
Final volume	**25 µl**

PCR condition			
	95°C	3 min	
	95°C	45 sec	35 x
	61°C	45 sec	
	72°C	1,5 min	
	72°C	10 min	

5.5.3 Agarose gel electrophoresis

The PCR products were analyzed by electrophoresis on agarose gel. The agarose was dissolved in 0.5x TBE and 5µl of ethidiumbromide (10mg/ml) were added to 100 ml of dissolved gel. For the PCR products a 1.5% agarose gel was used. As a marker 2.5 µl of Smartladder (EUROGENTEC) were also loaded on the gel to define the size of DNA bands. All samples contained 1xloading solution when loaded to the gel.

5.6 RNA analysis – in situ hybridization

5.6.1 Synthesis of digoxigenin (DIG) -labeled RNA-probes

The generation of single-stranded digoxigenin(DIG)-labeled RNA-probes was performed by in vitro transcription of a DNA-template. As template served a linearized plasmid; containing the appropriate sequence and promoters for RNA-polymerases flanking the probe sequence. Depending on the orientation of the probe sequence and the plasmid either T7 or SP6 was used to generate the anti-sense probe. The sense probe was synthesized using the other RNA-polymerase.

5.6.2 Synthesis of riboprobes by using PCR products as template

The DNA obtained was used for a PCR with M13 primers, contained in the vector, in order to amplify the cloned DAT fragment within.

M13 PCR	
10x buffer with $MgCl_2$	2 µl
dNTP (10 mM)	0,5 µl
Primer M13 forward (10 pM)	2 µl
Primer M13 reverse (10 pM)	2 µl
Taq-polymerase (1 U/µl)	0,5 µl
Sterile water	12 µl
DNA (Plasmid preparation 100 ng/µl)	1 µl

PCR		
95°C	**4 min**	
95°C	**30 sec**	**35 x**
63°C	**30 min**	
72°C	**30 min**	
72°C	**7 min**	

The amplified DNA was used (without purification) for the in vitro transcription. To label the RNA, a DIG RNA Labeling Mix, 10x conc. (from Roche) was used. Digoxigenin-UTP is incorporated by SP6 or T7 RNA polymerase at approximately every 20-25th nucleotide of the transcript under the conditions described below:

In vitro translation	
DNA (not purified PCR product)	1 μl
10x transcription buffer Roche	2 μl
DTT 100 mM	2 μl
10x RNA labelling mix (Roche)	2 μl
RNase inhibitor (Roche)	1 μl
T7, Sp6 RNA polymerase (Roche) (20 U/μl)	1 μl
DEPC water	11 μl
Final volume	20 μl

This reaction was incubated for 2 hours at 37°C. To digest the DNA template 2 μl of DNase I (10 U/μl) were added to each tube and left at 37°C for 15 min. The synthesized RNA was added with 30 μl of DEPC- H_2O and kept in ice. To purify the riboprobes from the not incorporated components, G50 spin columns were used. The lid and the tip are removed and the columns were centrifuged. The transcription mixture is loaded to the middle of the column and centrifuged 2 min at 3500 rpm. The flow-through is recovered, 4 μl of this are used to check the quality of the probe on a denaturating RNA gel and other 2 μl are used to check the yield of the RNA synthesis.

5.6.3 Denaturating RNA gel

For 50 ml of the gel 0,6g of agarose were diluted in 5 ml of MOPS and 37,5ml of DEPC-treated H_2O. The agarose was dissolved by microwave for 3 min at 600 watt, cooled down to 40°-50°C and 7,5ml of formaldehyde were added. The gel was poured in RNase free apparatus for electrophoresis. For 4 μl of sample, 12 μl of RNA loading buffer were used to load the sample in the gel. As a marker an already labeled control RNA (from the RNA labeling kit; Roche) was used in different concentrations.
The electrophoresis buffer was 1x MOPS, which was diluted from 10x MOPS with DEPC-treated H_2O.

5.6.4 RNA dot blot

To define the exact amount of the RNA probes, serial dilutions of the purified riboprobe were made. This was also done with the already labeled control RNA, which has the concentration of 100 ng/µl. 1µl of the labeled probe and diluted control RNA is spotted on a nylon membrane. The nucleic acids were fixed by cross-linking with UV-light (Stratalinker UV 1800, Stratagene) by using the auto crosslinking mode. The next step was to incubate the membrane with blocking solution (gentle shaken) for 30 min at RT. Anti-DIG alkaline phosphatase was diluted 1:5000 in blocking solution. The entire membrane had to be covered with the antibody dilution. After the incubation, the membrane was washed two times for 15 min with washing buffer. The washing buffer was removed and the color substrate of alkaline phosphatase BM purple (Roche) is added. The reaction was protected from light. After one hour the spots had a sufficient intensity the reaction was stopped by washing the membrane for five min in sterile water. To examine the amount of the labeled probes, the intensity of the diluted riboprobe was compared with the control.

5.6.5 In situ hybridization on paraffin sections

All solutions and equipment, used for the pre-hybridization steps should be RNase free. Stock solutions are therefore treated with DEPC and diluted in DEPC water. The paraffin slides were dewaxed in xylene 2 times for 10 min. The dehydration of the sections is done, by using a decreasing EtOH series: two times 5 min in 100% Ethanol and then 95%, 70%, 50% and 30% ethanol for 1 min each. Finally, they were washed two times for 5 min in PBS. To post-fix the sections 4% PFA was used for 20 min. Then the slides were washed two times 5 min in PBS. To make the RNA more accessible to the riboprobes, the slides were incubated with proteinase K solution for 6 min 30 seconds. Proteinase K solution was washed with PBS for 5min. The sections were fixed again in 4% PFA solution for 30 min. Two washing steps with PBS for 5 min

followed and another two times for 2 min in 2x SSC. The sections were left in Tris/Glycine buffer for 30 min.

Hybridization mix:

Hybridization mix	Final conc.	100 µl/slide
100% formamide	40%	40 µl
20x SSC pH 4,5	5x	25 µl
50x Denhardt's	1x	2 µl
10 mg/ml salmon sperm DNA	100 µg/ml	1 µl
10 mg/ml tRNA	100 µg/ml	1 µl
H_2O DEPC treated		30,9-30,8 µl
Probe	100 ng/ml	0,1-0,2 µl

The hybridization mix was heated at 95°C for 2 min and chilled on ice until use. The slides are incubated with 100 µl of hybridization mix and covered with slide-size cut parafilm. The slides were put on a grid into a plastic box with paper soaked with 5xSSC, 40% formamide and incubated over-night at 55°C. On the following day all solutions should be sterile but not necessarily to be RNase free. The solutions for all 37°C and 60°C washing steps should be pre-warmed.

NTE	SSC / formamide	Maleic acid solution
0,5 M NaCl 10 mM Tris pH 7,0 5 mM EDTA	0,5x SSC 20% formamide	11,61g of maleic acid dissolve in 800ml H_2O + 30 ml NaCl(10M) adjust pH to 7.5 with NaOH 10M adjust to 1l
prewarm to 37°C	prewarm to 60°C	

All room temperature washes are performed on a shaker. The parafilm was floated off with 5x SSC at RT. The sections were washed three times for 20 min in the same solution. In 0,5x SSC and 20% formamide the sections were washed at 60°C for 40 min. The solution was changed and placed at room temperature to cool down. Then the slides were equilibrated in NTE solution at 37°C for 15 min. Afterwards a second NTE wash for 30 min at 37°C with 10 μg/ml RNase, to remove the unspecific riboprobe binding. After a washing step for 15 min at 37°C in NTE, and 0,5x SSC and 20% formamide for 30 min at 60°C, finally the sections were washed in 2x SSC for 30 min at room temperature.

The slides were incubated with a 1x blocking solution diluted in maleic acid/ NaCl solution. The antibody against digoxigenin conjugated with alkaline phosphatase is diluted 1:200 in blocking solution and the sections incubated over-night at 4 °C (again covered with slide-size cut parafilm).

The third day started with the removal of parafilm with 1xTBS.

10xTBS	**Tween /levamisole**
80g NaCl 2g KCl 250ml 1M Tris/HCl pH 7,5 add H_2O to 1 liter	**0,1% Tween-10** **0,5 mg/ml levamisole**

The slides were washed four times for 10 min and once for 20 min in TBS. Next step was to rinse them in 1x Tween/ Levamisol solution for 10 min. BM purple substrate (Roche) was added with Tween/ Levamisole 1x solution, in order to reduce the activity of endogenous phosphatases. The slides were stained in the dark. Afterwards slides were rinsed for 10 min in PBS with 1mM EDTA to stop the reaction. The sections were mounted with Kaiser`s glycerol gelatine.

5.7 Protein analysis

5.7.1 Preparation of vibratome sections

The adult mice were sacrificed by asphyxiation with CO_2 and the brains were dissected. The brains were fixed in 50ml cold 4% PFA, gently shake for 48h at 4°C. After this incubation, the brains were stored in 0.4% PFA at 4°C until use. Coronal sections with a thickness of 50µm were produced using a vibratome (Microm). The floating sections were stored in 0.4% PFA at 4°C.

5.7.2 Preparation of embryos for paraffin sections

The adult mice were sacrificed by asphyxiation with CO_2 and the brains were dissected. The embryos were fixed in 50ml cold 4% PFA, gently shake overnight at 4°C. The following day the brains were washed two times for one hour with saline solution (0,83% NaCl solution), then treated with a washing solution containing a mix of saline solution and EtOH 95% with the ratio of 1:1, for one hour and finally washed with EtOH 70% two times for 60 min. All washing steps were done at RT. Afterwards the samples could be stored at 4°C for a longer period or further processed to paraffin embedding. We left the tissue at least over-night in 70% EtOH. Then they were washed with an EtOH-series (85%, 90% and 100%) each one half an hour and at RT. After the washing steps the solution (100% EtOH) was changed and the samples were placed over-night in 100% EtOH at 4°C, gently shaken. Next day: Tissue were transferred into xylene, washed two times for 1 hour (gently shaken at RT), then incubated with a mix of xylene and paraffin (ratio 1:1) for 1 hour at 60°C using a Tissue Tek Thermal console and Dispensing console (Miles Scientific). As embedding material “Gewebeeinbettungsmaterial Vogel-Histo Comp” (Vogel) was used. Three further steps with paraffin for 60 min at 60°C followed. Then the tissue was ready to be oriented and embedded in a paraffin block (using peel-a-way disposable plastic tissue embedding moulds from Polyscience, Inc.). The paraffin blocks were stored at 4°C until further use. For sections, a microtome 2035 from Leica Instruments was used. The paraffin block was fixed to the microtome and sections were cut with a

thickness of 7 μm. In order to flatten the sections, they were transfered in a histobath (HI1210, Leica Instruments). During the incubation (floating in water at 40°C for 10 min) the sections become more flat, scratches are removed and the tissue distended. The sections were collected on Superfrost slides, dried over-night at 37°C and then stored at RT.

5.7.3 Preparation of tissue for cryosections

The adult mice were sacrificed by asphyxiation with CO_2 and the brains were dissected. The brains were fixed in 50ml cold 30% sucrose/PBS. Then the embryos were rinsed in PBS, embedded in OCT Tissue Tek (Sakura Finetek, Netherlands), frozen in dry ice and stored at –80°C.

For frozen sections a cryostat CM 3050 from Leica Instruments was used. Samples were fixed to the object with Tissue Tek. The object temperature and the chamber temperature of the cryostat were set to –20°C. The thickness of the sections was 20μm. Continuous cutting mode with 30-60% speed was used. The sections were collected on Superfrost slides (Fisher Scientific, USA) and stored at –20°C.

5.8 Immunohistochemistry

5.8.1 Immunohistochemistry using paraffin sections

Paraffin sections were de-paraffinized 3x for 10min in xylene and hydrated through a decreasing ethanol gradient 2x5min $EtOH_{abs}$, 2x5min 95% EtOH, 2x5min 70% EtOH and 1x10min PBS. The antigen retrieval was performed by microwave treatment (3min 800W, 8min360W) in 1x Antigen Retrieval Citra buffer (Biogentex). The cooled sections were rinsed 3x in H_2O_{dd} and 3x in PBS. Afterwards the endogenous peroxidase activity was blocked by 10min incubation in 5% H_2O_2 diluted in PBS/MetOH (1:1) at RT followed by washing in PBS. Sections were rinsed 3x5min in PBS, circled with Pap-Pen (Beckman Coulter) and incubated for 30min with blocking solution (5% normal swine serum; DAKO in PBS) in a humid chamber. Incubation with the first antibody

was performed at 4°C O/N. Sections were rinsed next day 3x10min in PBS and afterwards incubated for 30 min with the appropriate biotinylated secondary antibody (Vector). After 3x10min rinsing in PBS, 30min incubation with the VECTSTAIN ABC system was performed according to the instruction of the manufacturer (streptavidin-biotin-complex coupled with horse radish peroxidase; Vector Laboratories). The sections were stained with 3,3-diaminobenzidine (DAB, Sigma) dissolved in H_2O. Replacing the DAB with tab water stopped the reaction, the sections were dehydrated by an increasing ethanol gradient (H_2Odd, 70% EtOH, 95% EtOH and $EtOH_{abs}$) followed by incubation in xylene and mounted with Eukitt (O.Kindler).

Following primary antibodies were used:

Cre	1:2000
TH	1:500
B23	1:2000
p53	1:1000
8-oxoguanine	1:200
Neuroketals	1:1000
NITT	1:1000
Parkin	1:500
Ubiquitin	1:3000
Synphilin	1:500
α-synuclein	1:5000

5.8.2 Immunohistochemistry using vibratome sections

Free floating vibratome sections were transferred into a 48 well plate containing PBS and endogenous peroxidase activity was blocked by 15 min incubation in 1% H_2O_2 diluted in PBS/MetOH (1:1). Subsequently, sections were rinsed 3x 10min in PBST followed by 30min incubation in 5% NSS/PBST to block unspecific binding sites. Incubation with the first antibody, appropriately diluted in 5% NSS/PBST, was performed O/N at 4°C. After rinsing 3x15 min in PBST the sections were incubated for 30 min at RT with the adequate biotinylated secondary antibody (Vector) and rinsed again 3x15 min with PBST. 30min incubation with the VECTASTAIN ABC system was performed according to the instruction of the manufacturer (streptavidin-biotin-

complex coupled with horse radish peroxidase; Vector). Sections were finally rinsed 2x15min with PBST and 2x15min with PBS. The sections were stained with either 3,3-diaminobenzidine (DAB;Sigma) or with Histogreen (Vector). The reaction was stopped with tap water onto uncoated glass slides. Sections were dried for 1 hr at RT, shortly dipped into xylene and mounted with Eukitt (O. Kindler)

Following primary antibodies were used:

Cre	1:3000
TH	1:2000
B23	1:2000

5.8.3 Immunoflorescence using paraffin sections

Paraffin sections were de-paraffinized 3x for 10 min in xylene and hydrated through a decreasing ethanol gradient 2x5 min $EtOH_{abs}$, 2x5 min 95% EtOH, 2x5 min 70% EtOH and 1x10 min PBS. The antigen retrieval was performed by microwave treatment (3 min 800W, 8 min 360W) in 1x Antigen Retrieval Citra buffer (Biogentex). The cooled sections were rinsed 3x in H_2Odd and 3x in PBS. Sections were rinsed 3x5 min in PBS, circled with Pap-Pen (Beckman Coulter) and incubated for 30 min with blocking solution (5% normal swine serum; DAKO in PBS) in a humid chamber. Incubation with the first antibody was performed at 4°C O/N. Sections were rinsed next day 3x10 min in PBS and afterwards incubated for 30 min with the appropriate fluorescent secondary antibody (Molecular Probes). After 3x10 min rinsing in PBS section were mounted with Vectashield mounting material (with or without DAPI).

Following primary antibodies were used:

TH	1:200
Cre	1:200
B23	1:200

5.8.4 COX staining using cryosections

The sections were dried for 20-30 min at RT. After rinsing with PBS dections were stained using cresylviolett for max. 1 min. Sections were rinsed with PBS, followed by 10 min incubation in COX buffer at RT (gently shaking). Sections were stained using COX reaction mix for 30-40 min at 37°C. Reaction was stopped by rinsing the sections 3x for 3min with COX buffer. Sections were dehydrated in an increasing ethanol gradient (H_2O_{dd}, 70% EtOH, 95% EtOH and $EtOH_{abs}$) followed by incubation in xylene and mounted with Eukitt (O. Kindler).

COX buffer
50mM sodium phosphate pH 7.2
200mg/ml sucrose

COX reaction mix
50mM sodium phosphate pH 7.2
10mg/ml cytochrome c
10mg/ml DAB
200mg/ml sucrose
catalase 1.600U/ml

5.8.5 Hematoxylen/eosin staining of paraffin sections

For hemaloxylen/eosin staining, paraffin sections with a thickness of 4µm were deparaffinized 2x for 5min in xylene and hydrated through a decreasing ethanol gradient (2x3min $EtOH_{abs}$, 2x3min 95%EtOH, 2x3min 70%EtOH and 3min tap water) followed by 5min incubation in Mayers hemalaun (Applichem), 1min in 0.5% HCl in 70%EtOH and 5min treatment with running tap water to differentiate the signal. Sections were counter-stained for 1min with eosin (Sigma), washed in H_2O_{dd} and dehydrated through an increasing ethanol gradient (H_2O_{dd}, 3min 80%EtOH and 2x2min $EtOH_{abs}$). After 2x5min incubation in xylene, the sections were mounted with Eukitt (O.Kindler).

Eosin staining solution

30ml	1% Eosin
270ml	70%EtOH
3ml	glacial acetic acid

5.8.6 ß-galactosidase staining

For β-galactosidase whole mount staining, dissected brains were cut with a razor blade in the appropriate planes. The organs were rinsed 3x for 10min with washing buffer and subsequently stained with X-gal staining solution at 37°C over night. After the staining, slices were postfixed with 4% paraformaldehyde at 4°C over night and kept in 1xPBS at 4°C for analysis. For β-galactosidase staining of cryosections, dissected brains were frozen in O.C.T. compound (Tissue Tek, Sakura Finetek) on ethanol/dry ice and 10µm sagital cryosections were prepared (cryostat – Leica). Sections were fixed for 10min in 4% paraformaldehyde and β-galactosidase staining was performed as described for whole mount samples. Afterwards, sections were counterstained with nuclear fast red (Sigma) and mounted with Eukitt (O.Kindler).

<u>washing buffer</u>
5mM EGTA
2mM $MgCl_2$
0.01% sodium-deoxycholat
0.02% NP-40
solved in PBS

<u>X-gal staining solution</u>
5mM EGTA, pH8
2mM $MgCl_2$
0.01% sodium-deoxycholat
0.02% NP-40
10mM $K_3[Fe(CN)_6]$
10mM $K_4[Fe(CN)_6]$
0.5mg/ml X-gal (50mg/ml in dimethylformamide; Applichem) solved in PBS

5.8.7 HPLC-Electrochemical Detection

For measurements of dopamine release, control and mutant mice were sacrificed at P40, the striata were frozen in liquid nitrogen. After weighing, the tissue was homogenized in 300µl 20mM sodium acetate buffer with 0,1% Trition-X-100. An aliquot was processed for analysis of dopamine. An 100µl aliquot was added to 900µl of 0,1M sodium acetate buffer containing 1%

Trition-X-100, 25mM ethylenediaminotetraacetic acid (EDTA) and as internal standard N-methyl-dopamine. Following deproteinization with 50µl $HClO_4$ (70%) and centrifugation. 100µl of the supernatant were processed by alumina extraction in triplicate. Dopamine was detected by HPLC-ED (µ-Bondapack-C18 column, 10µm particle size, Waters system with pump 510; sample processor 740; Metrohom amperometric detector with glassy carbon electrodes at a potential of 0.72V against an Ag/AgCl reference electrode) and quantified by comparison to the internal standard. Elution was performed with 50mM $HClO_4$ containing 25mM EDTA at a flow rate of 1-1,2ml/min. Homogenates were processed for dopamine determination by HPLC-ED as described (Otto and Unsicker, 1990).

5.8.8 Quantitative analysis of dopaminergic neurons

Total numbers of TH positive neurons in SN and VTA, identified according to established anatomical landmarks, were counted on more than 20 sections per animal, immunostained with TH antibody. In the case of double immunohistochemistry every 4^{th} section was used for cell counting spanning the entire region containing dopaminergic neurons. For each experimental group at least 3 mice were used. The ImageJ program (http://rsb.info.nih.gov/ij/) was used to determine the optical density of TH signal in the striata of control and mutant mice. Statistical analysis was performed by using the GraphPad Prism program (GraphPad, USA). Statistical significance was assessed by Students t-test, one-way ANOVA or two-way ANOVA. P values are expressed in comparison to respective control (*, $p<0.05$; **, $p<0.01$; ***, $p<0.001$).

5.9 Mouse work

5.9.1 C57/Bl6

This strain is bred by Charles River Laboratories (Wilmington, USA). These mice were used to backcross the generated transgenic lines. Mice are kept in a pathogen-free facility with a 12 hours light-dark cycle and water/food ad libitum

5.9.2 Tamoxifen treatment

Tamoxifen (Sigma) was dissolved in sunflower seed oil/ethanol (10:1) mixture at a final concentration of 10mg/ml. Eight weeks old mice were injected intraperitoneally with 1mg of tamoxifen twice a day for 5 consecutive days. Vehicle-treated animals were injected with 100µl of sunflower seed oil/ethanol mixture.

Tamoxifen: 50mg tamoxifen (Sigma) was added to 500µl $EtOH_{abs}$ plus 4,5ml sunflower seed oil (Sigma) and dissolved under slow rotation for about 2hrs at RT. After tamoxifen solved it was stored at 4°C for up to three days.

5.9.3 MPTP

Adult mice received 3 intraperitoneal injections of 30mg/kg MPTP hydrochloride (Sigma) dissolved in 0,5ml of 0,9% saline adjusted to pH 7,4 at 24hrs intervals. In the case of the TIF-$IA^{DATCreERT2}$ mice the first injection was given 2 weeks after the tamoxifen treatment. Control mice received injections of saline according to the same protocol (Schober, et al., 2007).

5.9.4 Treatment with L-DOPA

Treatment of mice with L-DOPA was performed as described (Szczypka, et al., 2001). Mice were weighed daily, and afterwards injected with L-DOPA (50mg/kg) consisting of 1,5mg/ml L-DOPA dissolved in 2,5mg/ml ascorbic acid. In addition liquid food, which is easier accessible, was provided.

5.9.5 Implantation of dopamine pellets

Pellets, containing a biodegradable matrix, that effectively and continuously releases dopamine (1mg/day) for 30 days (Innovated Research of America), were implanted subcutaneously in the animal.

5.9.6 Behavioral assessment

One week before the experimental period, mutant and control male mice were transferred to standard single mouse cages. All results are represented as mean +/- SEM. The genotype effect was analyzed using unpaired two-tailed Student's t test or two-way ANOVA using the Prism computer program.

5.9.7 Rotarod

Motor coordination measurements were done on the rotating drum with accelerated speed (Accelerator: Rotarod, Jones & Roberts, for mice 7650, TSE). After 10min adaptation at 2,5 rpm, the time the animal spent on the accelerating rod was recorded.

6. Literature

Abou-Sleiman, P. M., Muqit, M. M. and Wood, N. W. (2006) Expanding insights of mitochondrial dysfunction in Parkinson's disease. *Nat Rev Neurosci* **7**:207-19.

Ahlskog, J. E. and Muenter, M. D. (2001) Frequency of levodopa-related dyskinesias and motor fluctuations as estimated from the cumulative literature. *Mov Disord* **16**:448-58.

Alves da Costa, C., Sunyach, C., Pardossi-Piquard, R., Sevalle, J., Vincent, B., Boyer, N., Kawarai, T., Girardot, N., St George-Hyslop, P. and Checler, F. (2006) Presenilin-dependent gamma-secretase-mediated control of p53-associated cell death in Alzheimer's disease. *J Neurosci* **26**:6377-85.

Bae, B. I., Xu, H., Igarashi, S., Fujimuro, M., Agrawal, N., Taya, Y., Hayward, S. D., Moran, T. H., Montell, C., Ross, C. A., Snyder, S. H. and Sawa, A. (2005) p53 mediates cellular dysfunction and behavioral abnormalities in Huntington's disease. *Neuron* **47**:29-41.

Bender, A., Krishnan, K. J., Morris, C. M., Taylor, G. A., Reeve, A. K., Perry, R. H., Jaros, E., Hersheson, J. S., Betts, J., Klopstock, T., Taylor, R. W. and Turnbull, D. M. (2006) High levels of mitochondrial DNA deletions in substantia nigra neurons in aging and Parkinson disease. *Nat Genet* **38**:515-7.

Benes, F. M. (2001) Carlsson and the discovery of dopamine. *Trends Pharmacol Sci* **22**:46-7.

Bernoud-Hubac, N., Davies, S. S., Boutaud, O., Montine, T. J. and Roberts, L. J., 2nd (2001) Formation of highly reactive gamma-ketoaldehydes (neuroketals) as products of the neuroprostane pathway. *J Biol Chem* **276**:30964-70.

Bier, E. (2006) Antioxidants put Parkinson flies back in the PINK. *Proc Natl Acad Sci U S A* **103**:13269-70.

Birkmayer, W. and Hornykiewicz, O. (1961) [The L-3,4-dioxyphenylalanine (DOPA)-effect in Parkinson-akinesia.]. *Wien Klin Wochenschr* **73**:787-8.

Bodem, J., Dobreva, G., Hoffmann-Rohrer, U., Iben, S., Zentgraf, H., Delius, H., Vingron, M. and Grummt, I. (2000) TIF-IA, the factor mediating growth-dependent control of ribosomal RNA synthesis, is the mammalian homolog of yeast Rrn3p. *EMBO Rep* **1**:171-5.

Boisvert, F. M., van Koningsbruggen, S., Navascues, J. and Lamond, A. I. (2007) The multifunctional nucleolus. *Nat Rev Mol Cell Biol* **8**:574-85.

Buttgereit, D., Pflugfelder, G. and Grummt, I. (1985) Growth-dependent regulation of rRNA synthesis is mediated by a transcription initiation factor (TIF-IA). *Nucleic Acids Res* **13**:8165-80.

Candy, J. M., Perry, R. H., Perry, E. K., Irving, D., Blessed, G., Fairbairn, A. F. and Tomlinson, B. E. (1983) Pathological changes in the nucleus of Meynert in Alzheimer's and Parkinson's diseases. *J Neurol Sci* **59**:277-89.

Carlsson, A., Lindqvist, M. and Magnusson, T. (1957) 3,4-Dihydroxyphenylalanine and 5-hydroxytryptophan as reserpine antagonists. *Nature* **180**:1200.

Casanova, E., Fehsenfeld, S., Mantamadiotis, T., Lemberger, T., Greiner, E., Stewart, A. F. and Schutz, G. (2001) A CamKIIalpha iCre BAC allows brain-specific gene inactivation. *Genesis* **31**:37-42.

Cavanaugh, A. H., Hirschler-Laszkiewicz, I., Hu, Q., Dundr, M., Smink, T., Misteli, T. and Rothblum, L. I. (2002) Rrn3 phosphorylation is a regulatory checkpoint for ribosome biogenesis. *J Biol Chem* **277**:27423-32.

Cenci, M. A. (2007) Dopamine dysregulation of movement control in L-DOPA-induced dyskinesia. *Trends Neurosci* **30**:236-43.

Conforti, L., Adalbert, R. and Coleman, M. P. (2007) Neuronal death: where does the end begin? *Trends Neurosci* **30**:159-66.

Cummings, C. J., Reinstein, E., Sun, Y., Antalffy, B., Jiang, Y., Ciechanover, A., Orr, H. T., Beaudet, A. L. and Zoghbi, H. Y. (1999) Mutation of the E6-AP ubiquitin ligase reduces nuclear inclusion frequency while accelerating polyglutamine-induced pathology in SCA1 mice. *Neuron* **24**:879-92.

Dauer, W. and Przedborski, S. (2003) Parkinson's disease: mechanisms and models. *Neuron* **39**:889-909.

Ekstrand, M. I., Terzioglu, M., Galter, D., Zhu, S., Hofstetter, C., Lindqvist, E., Thams, S., Bergstrand, A., Hansson, F. S., Trifunovic, A., Hoffer, B., Cullheim, S., Mohammed, A. H., Olson, L. and Larsson, N. G. (2007) Progressive parkinsonism in mice with respiratory-chain-deficient dopamine neurons. *Proc Natl Acad Sci U S A* **104**:1325-30.

Erdmann, G., Schutz, G. and Berger, S. (2007) Inducible gene inactivation in neurons of the adult mouse forebrain. *BMC Neurosci* **8**:63.

Feil, R., Wagner, J., Metzger, D. and Chambon, P. (1997) Regulation of Cre recombinase activity by mutated estrogen receptor ligand-binding domains. *Biochem Biophys Res Commun* **237**:752-7.

Finkel, T. (2005) Opinion: Radical medicine: treating ageing to cure disease. *Nat Rev Mol Cell Biol* **6**:971-6.

Forman, M. S., Lee, V. M. and Trojanowski, J. Q. (2005) Nosology of Parkinson's disease: looking for the way out of a quagmire. *Neuron* **47**:479-82.

German, D. C. and Manaye, K. F. (1993) Midbrain dopaminergic neurons (nuclei A8, A9, and A10): three-dimensional reconstruction in the rat. *J Comp Neurol* **331**:297-309.

Giorgio, M., Migliaccio, E., Orsini, F., Paolucci, D., Moroni, M., Contursi, C., Pelliccia, G., Luzi, L., Minucci, S., Marcaccio, M., Pinton, P., Rizzuto, R., Bernardi, P., Paolucci, F. and Pelicci, P. G. (2005) Electron transfer between cytochrome c and p66Shc generates reactive oxygen species that trigger mitochondrial apoptosis. *Cell* **122**:221-33.

Goldman, J. E., Yen, S. H., Chiu, F. C. and Peress, N. S. (1983) Lewy bodies of Parkinson's disease contain neurofilament antigens. *Science* **221**:1082-4.

Graham, D. G., Tiffany, S. M., Bell, W. R., Jr. and Gutknecht, W. F. (1978) Autoxidation versus covalent binding of quinones as the mechanism of toxicity of dopamine, 6-hydroxydopamine, and related compounds toward C1300 neuroblastoma cells in vitro. *Mol Pharmacol* **14**:644-53.

Grewal, S. S., Evans, J. R. and Edgar, B. A. (2007) Drosophila TIF-IA is required for ribosome synthesis and cell growth and is regulated by the TOR pathway. *J Cell Biol* **179**:1105-13.

Halliwell, B. (1992) Reactive oxygen species and the central nervous system. *J Neurochem* **59**:1609-23.

Indra, A. K., Warot, X., Brocard, J., Bornert, J. M., Xiao, J. H., Chambon, P. and Metzger, D. (1999) Temporally-controlled site-specific mutagenesis in the basal layer of the epidermis: comparison of the recombinase activity of the tamoxifen-inducible Cre-ER(T) and Cre-ER(T2) recombinases. *Nucleic Acids Res* **27**:4324-7.

Kashihara, K. (2007) Management of levodopa-induced dyskinesias in Parkinson's disease. *J Neurol* **254 Suppl 5**:27-31.

Kern, D. S. and Kumar, R. (2007) Deep brain stimulation. *Neurologist* **13**:237-52.

Kim, R. H., Smith, P. D., Aleyasin, H., Hayley, S., Mount, M. P., Pownall, S., Wakeham, A., You-Ten, A. J., Kalia, S. K., Horne, P., Westaway, D., Lozano, A. M., Anisman, H., Park, D. S. and Mak, T. W. (2005a) Hypersensitivity of DJ-1-deficient mice to 1-methyl-4-phenyl-1,2,3,6-tetrahydropyrindine (MPTP) and oxidative stress. *Proc Natl Acad Sci U S A* **102**:5215-20.

Kim, R. H., Peters, M., Jang, Y., Shi, W., Pintilie, M., Fletcher, G. C., DeLuca, C., Liepa, J., Zhou, L., Snow, B., Binari, R. C., Manoukian, A. S., Bray, M. R., Liu, F. F., Tsao, M. S. and Mak, T. W. (2005b) DJ-1, a novel regulator of the tumor suppressor PTEN. *Cancer Cell* **7**:263-73.

Kruhlak, M., Crouch, E. E., Orlov, M., Montano, C., Gorski, S. A., Nussenzweig, A., Misteli, T., Phair, R. D. and Casellas, R. (2007) The ATM repair pathway inhibits RNA polymerase I transcription in response to chromosome breaks. *Nature* **447**:730-4.

Kurki, S., Peltonen, K., Latonen, L., Kiviharju, T. M., Ojala, P. M., Meek, D. and Laiho, M. (2004) Nucleolar protein NPM interacts with HDM2 and protects tumor suppressor protein p53 from HDM2-mediated degradation. *Cancer Cell* **5**:465-75.

Lang, A. E. and Lozano, A. M. (1998a) Parkinson's disease. Second of two parts. *N Engl J Med* **339**:1130-43.

Lang, A. E. and Lozano, A. M. (1998b) Parkinson's disease. First of two parts. *N Engl J Med* **339**:1044-53.

Lee, E. C., Yu, D., Martinez de Velasco, J., Tessarollo, L., Swing, D. A., Court, D. L., Jenkins, N. A. and Copeland, N. G. (2001) A highly efficient Escherichia coli-based chromosome engineering system adapted for recombinogenic targeting and subcloning of BAC DNA. *Genomics* **73**:56-65.

Lin, M. T. and Beal, M. F. (2006) Mitochondrial dysfunction and oxidative stress in neurodegenerative diseases. *Nature* **443**:787-95.

Lindvall, O. and Kokaia, Z. (2006) Stem cells for the treatment of neurological disorders. *Nature* **441**:1094-6.

Lohrum, M. A., Ludwig, R. L., Kubbutat, M. H., Hanlon, M. and Vousden, K. H. (2003) Regulation of HDM2 activity by the ribosomal protein L11. *Cancer Cell* **3**:577-87.

Lotharius, J. and Brundin, P. (2002) Pathogenesis of Parkinson's disease: dopamine, vesicles and alpha-synuclein. *Nat Rev Neurosci* **3**:932-42.

Mayer, C. and Grummt, I. (2005) Cellular stress and nucleolar function. *Cell Cycle* **4**:1036-8.

Mayer, C., Bierhoff, H. and Grummt, I. (2005) The nucleolus as a stress sensor: JNK2 inactivates the transcription factor TIF-IA and down-regulates rRNA synthesis. *Genes Dev* **19**:933-41.

Michel, P. P., Ruberg, M. and Hirsch, E. (2006) Dopaminergic neurons reduced to silence by oxidative stress: an early step in the death cascade in Parkinson's disease? *Sci STKE* **2006**:pe19.

Moore, D. J., Dawson, V. L. and Dawson, T. M. (2006) Lessons from Drosophila models of DJ-1 deficiency. *Sci Aging Knowledge Environ* **2006**:pe2.

Moore, D. J., West, A. B., Dawson, V. L. and Dawson, T. M. (2005) Molecular pathophysiology of Parkinson's disease. *Annu Rev Neurosci* **28**:57-87.

Nair, V. D., McNaught, K. S., Gonzalez-Maeso, J., Sealfon, S. C. and Olanow, C. W. (2006) p53 Mediates non-transcriptional cell death in dopaminergic cells in response to proteasome inhibition. *J Biol Chem* **281**:39550-60.

Olson, M. O., Hingorani, K. and Szebeni, A. (2002) Conventional and nonconventional roles of the nucleolus. *Int Rev Cytol* **219**:199-266.

Orsini, F., Migliaccio, E., Moroni, M., Contursi, C., Raker, V. A., Piccini, D., Martin-Padura, I., Pelliccia, G., Trinei, M., Bono, M., Puri, C., Tacchetti, C., Ferrini, M., Mannucci, R., Nicoletti, I., Lanfrancone, L., Giorgio, M. and Pelicci, P. G. (2004) The life span determinant p66Shc localizes to mitochondria where it associates with mitochondrial heat shock protein 70 and regulates trans-membrane potential. *J Biol Chem* **279**:25689-95.

Otto, D. and Unsicker, K. (1990) Basic FGF reverses chemical and morphological deficits in the nigrostriatal system of MPTP-treated mice. *J Neurosci* **10**:1912-21.

Parkinson, J. (2002) An essay on the shaking palsy. 1817. *J Neuropsychiatry Clin Neurosci* **14**:223-36; discussion 222.

Parlato, R., Rieker, C., Turiault, M., Tronche, F. and Schutz, G. (2006) Survival of DA neurons is independent of CREM upregulation in absence of CREB. *Genesis* **44**:454-464.

Przedborski, S. and Vila, M. (2003) The 1-methyl-4-phenyl-1,2,3,6-tetrahydropyridine mouse model: a tool to explore the pathogenesis of Parkinson's disease. *Ann N Y Acad Sci* **991**:189-98.

Rubbi, C. P. and Milner, J. (2003) Disruption of the nucleolus mediates stabilization of p53 in response to DNA damage and other stresses. *Embo J* **22**:6068-77.

Saudou, F., Finkbeiner, S., Devys, D. and Greenberg, M. E. (1998) Huntingtin acts in the nucleus to induce apoptosis but death does not correlate with the formation of intranuclear inclusions. *Cell* **95**:55-66.

Schedl, A., Larin, Z., Montoliu, L., Thies, E., Kelsey, G., Lehrach, H. and Schutz, G. (1993) A method for the generation of YAC transgenic mice by pronuclear microinjection. *Nucleic Acids Res* **21**:4783-7.

Schnapp, A., Pfleiderer, C., Rosenbauer, H. and Grummt, I. (1990) A growth-dependent transcription initiation factor (TIF-IA) interacting with RNA polymerase I regulates mouse ribosomal RNA synthesis. *Embo J* **9**:2857-63.

Schober, A. (2004) Classic toxin-induced animal models of Parkinson's disease: 6-OHDA and MPTP. *Cell Tissue Res* **318**:215-24.

Schober, A., Peterziel, H., von Bartheld, C. S., Simon, H., Krieglstein, K. and Unsicker, K. (2007) GDNF applied to the MPTP-lesioned nigrostriatal system requires TGF-beta for its neuroprotective action. *Neurobiol Dis* **25**:378-91.

Shimshek, D. R., Kim, J., Hubner, M. R., Spergel, D. J., Buchholz, F., Casanova, E., Stewart, A. F., Seeburg, P. H. and Sprengel, R. (2002) Codon-improved Cre recombinase (iCre) expression in the mouse. *Genesis* **32**:19-26.

Soriano, P. (1999) Generalized lacZ expression with the ROSA26 Cre reporter strain. *Nat Genet* **21**:70-1.

St-Pierre, J., Drori, S., Uldry, M., Silvaggi, J. M., Rhee, J., Jager, S., Handschin, C., Zheng, K., Lin, J., Yang, W., Simon, D. K., Bachoo, R. and Spiegelman, B. M. (2006) Suppression of reactive oxygen species and neurodegeneration by the PGC-1 transcriptional coactivators. *Cell* **127**:397-408.

Storz, P. (2006) Reactive oxygen species-mediated mitochondria-to-nucleus signaling: a key to aging and radical-caused diseases. *Sci STKE* **2006**:re3.

Sugimoto, M., Kuo, M. L., Roussel, M. F. and Sherr, C. J. (2003) Nucleolar Arf tumor suppressor inhibits ribosomal RNA processing. *Mol Cell* **11**:415-24.

Szczypka, M. S., Kwok, K., Brot, M. D., Marck, B. T., Matsumoto, A. M., Donahue, B. A. and Palmiter, R. D. (2001) Dopamine production in the caudate putamen restores feeding in dopamine-deficient mice. *Neuron* **30**:819-28.

Tao, W. and Levine, A. J. (1999) P19(ARF) stabilizes p53 by blocking nucleo-cytoplasmic shuttling of Mdm2. *Proc Natl Acad Sci U S A* **96**:6937-41.

Trimmer, P. A., Smith, T. S., Jung, A. B. and Bennett, J. P., Jr. (1996) Dopamine neurons from transgenic mice with a knockout of the p53 gene resist MPTP neurotoxicity. *Neurodegeneration* **5**:233-9.

Vila, M. and Przedborski, S. (2003) Targeting programmed cell death in neurodegenerative diseases. *Nat Rev Neurosci* **4**:365-75.

Vousden, K. H. and Lane, D. P. (2007) p53 in health and disease. *Nat Rev Mol Cell Biol* **8**:275-83.

Wise, R. A. (2004) Dopamine, learning and motivation. *Nat Rev Neurosci* **5**:483-94.

Yamamoto, R. T., Nogi, Y., Dodd, J. A. and Nomura, M. (1996) RRN3 gene of Saccharomyces cerevisiae encodes an essential RNA polymerase I transcription factor which interacts with the polymerase independently of DNA template. *Embo J* **15**:3964-73.

Yang, Y., Gehrke, S., Haque, M. E., Imai, Y., Kosek, J., Yang, L., Beal, M. F., Nishimura, I., Wakamatsu, K., Ito, S., Takahashi, R. and Lu, B. (2005) Inactivation of Drosophila DJ-1 leads to impairments of oxidative stress response and phosphatidylinositol 3-kinase/Akt signaling. *Proc Natl Acad Sci U S A* **102**:13670-5.

Yoshida, Y., Izumi, H., Torigoe, T., Ishiguchi, H., Itoh, H., Kang, D. and Kohno, K. (2003) P53 physically interacts with mitochondrial transcription factor A and differentially regulates binding to damaged DNA. *Cancer Res* **63**:3729-34.

Yuan, X., Zhou, Y., Casanova, E., Chai, M., Kiss, E., Grone, H. J., Schutz, G. and Grummt, I. (2005) Genetic inactivation of the transcription factor TIF-IA leads to nucleolar disruption, cell cycle arrest, and p53-mediated apoptosis. *Mol Cell* **19**:77-87.

Zhang, C., Comai, L. and Johnson, D. L. (2005) PTEN represses RNA Polymerase I transcription by disrupting the SL1 complex. *Mol Cell Biol* **25**:6899-911.

Zhao, J., Yuan, X., Frodin, M. and Grummt, I. (2003) ERK-dependent phosphorylation of the transcription initiation factor TIF-IA is required for RNA polymerase I transcription and cell growth. *Mol Cell* **11**:405-13.

7. Abbreviations

ERT2	LBD of the estrogen receptor harboring 2 pointmutations
EtOH	ethanol
h	hour
H_2O	water
H_2O_2	hydrogen peroxide
HCl	hydrochloric acid
Hsp	heatshock protein
IHC	immunohistochemistry
i.p.	intraperitoneal
kb	kilo base pair
Kferric	potassium hexacyanoferrat(II)trihydrate
Kferroc	potassium hexacyanferrat(III)
l	liter
LacZ	ß-galactosidase gene
LBD	ligand-binding domain
LoxP	Cre recombinase recognition site
µ	micro (10^{-6})
M	molar
mg	milligram
min	minute
ml	milliliter
mM	millimolar
mRNA	messenger- ribonucleic acid

n	nano (10^{-9})
NaCl	sodium chloride
NaOH	sodium hydroxide
NID	non-ionic detergent buffer
NP40	nonidet P40
PBS	phosphate buffered saline
PCR	polymerase chain reaction
PFA	paraformaldehyde
pH	pH-value
RNA	ribonucleic acid
RNase	ribonuclease
rpm	rounds per minute
RT	room temperature
s	second
SDS	sodiumdodecylsulfate
TAE	tris acetate EDTA buffer
TBE	tris borate EDTA buffer
TE	tris EDTA
TH	tyrosine hydroxylase
wt	wildtype
X-gal	5-bromo-4-chloro-3-indolyl-beta-D-galactopyranoside

8. Bibliography

Rieker, C., Parlato, R., Kreiner, G., Engblom, D., Schober, A., Stotz, S., Neumann, M., Yuan, X., Grummt, I. and Schütz, G. (2008) A novel function of the nucleolus: disruption of its activity in dopaminergic neurons leads to progressive parkinsonism. *Nature Medicine* (submitted).

Zwerts, F., Lupu, F., De Vriese, A., Pollefeyt, S., Moons, L., Altura, R. A., Jiang, Y., Maxwell, P. H., Hill, P., Oh, H., Rieker, C., Collen, D., Conway, S. J. and Conway, E. M. (2007) Lack of endothelial cell survivin causes embryonic defects in angiogenesis, cardiogenesis, and neural tube closure. *Blood* **109**:4742-52.

Rieker, C., Parlato, R., Turiault, M., Tronche, F. and Schutz, G. (2006) Survival of DA neurons is independent of CREM upregulation in absence of CREB. *Genesis* **44**:454-464.

9. Acknowledgements

I want to express my gratitude to Prof. Günther Schütz for the opportunity to work within his group and his continues encouragement. I also want to thank Prof. Dr. Hilmar Bading for serving as my second supervisor.
To all members past or present of the Schütz Lab, my friends and of course my family I owe you one.

And finally I want to dedicate this work to my grandpa, which unfortunately cannot be present when I finally get a real job!